PNNL-11790

Pacific Northwest
National Laboratory
Operated by Battelle for the
U.S. Department of Energy

Liquidus Temperature Data for DWPF Glass

TANK FOCUS AREA

TTP Number: RL3-7-WT-31, TFA Task 1

Optimization of Waste Loading in Glass

Milestone: 1B3

P. Hrma
J. D. Vienna
M. Mika
J. V. Crum
G. F. Piepel

May, 1999

Prepared for the U.S. Department of Energy
Under Contract DE-AC06-76RLO 1830

Pacific Northwest National Laboratory
Richland, Washington 99352

PNNL-11790

DISCLAIMER

PACIFIC NORTHWEST NATIONAL LABORATORY

operated by

BATTELLE MEMORIAL INSTITUTE

for the

UNITED STATES DEPARTMENT OF ENERGY

under Contract DE-AC06-76RLO 1830

Printed in the United States of America

Available to DOE and DOE contractors from the
Office of Scientific and Technical Information, P.O. Box 62, Oak Ridge, TN 37831;
prices available from (615) 576-8401.

Available to the public from the National Technical Information Service,
U.S. Department of Commerce, 5285 Port Royal Rd., Springfield, VA 22161

Summary

A liquidus temperature (T_L) database has been developed at the Pacific Northwest Laboratory (PNNL) for the Defense Waste Processing Facility (DWPF) glass composition region to support DWPF process control schemes. A test matrix consisting of 53 glasses (including two duplicates) was generated at the Savannah River Technology Center (SRTC) using statistical experimental design methods.

To ensure homogeneity, glasses were melted twice. Both melts were performed at $T = T_5 + \Delta T$, where T_5 is the temperature at which the melt viscosity is 5 Pa·s and $\Delta T \geq 100°C$. The T_5 value was estimated using a PNNL viscosity database. Its span for the test matrix was 1007°C to 1284°C. Melting at $T > T_5$ (from 1107°C to 1400°C) was necessary to dissolve (and possibly volatilize) some of the RuO_2. All glasses contained a large fraction of 0.09 mass% RuO_2, which prevented a reliable detection of spinel near the liquidus temperature (T_L) when the melting temperature was T_5.

T_L was measured by heat-treating glass samples over a range of constant temperatures. We used optical microscopy to detect the presence or absence of crystals in the samples. T_L was determined from observing crystallization within the bulk glass (more than 0.5 mm from the glass surface). The T_L values were adjusted by measuring the T_L of an internal PNNL standard glass in each furnace and checked by a National Bureau of Standards (NBS) standard glass. All measured T_L values are summarized in Table I-S.

The accuracy of values is estimated at ±10°C, based on the accuracy of calibrated thermocouples and the ability to discern spinel crystals in glass near T_L. Another possible source of error is glass redox connected with the difference between the melting temperature and T_L. The heat treatment period of samples was long enough to ensure equilibrating the glass with atmospheric air. However, repeated measurements of one of the DWPF glasses at the beginning and after the completion of the study shows that the actual accuracy of the T_L values may be in the ±12°C range. This error is small compared to the component effects (the difference between the lowest and highest T_L measured is $\Delta T_L = 523°C$).

Table I-S. Summary of Measured T_L Values (in °C) and Primary Crystallization Phases (PP)

	ID	T_L	PP[a]		ID	T_L	PP[a]		ID	T_L	PP[a]
1	SG01	1124	S	24	SG18	883	S	47	SG36	813	C
2	SG02	775	C	25	SG18	883	S	48	SG37	944	S
3	SG02	755	C	26	SG18	891	S	49	SG38	897	S
4	SG03	1164	S	27	SG18	882	S	50	SG39	1164	S
5	SG04	1261	S	28	SG19	929	S	51	SG40	1173	S
6	SG05	1084	S	29	SG20	799	S and C	52	SG41	1304	S
7	SG06	911	S	30	SG21	987	S	53	SG42	990	S
8	SG06	931	S	31	SG22	1145	S	54	SG43	924	S
9	SG06	929	S	32	SG23	1069	S	55	SG44	1244	S
10	SG07	950	S	33	SG24	995	C	56	SG45	936	S and C
11	SG08	1114	S	34	SG25	1310	S	57	SG46	1247	S
12	SG09	1173	S	35	SG25	1309	S	58	SG47	1144	S
13	SG10	1098	S	36	SG25	1296	S	59	SG48	862	C
14	SG11	895	S	37	SG26	1071	S	60	SG48	847	C
15	SG12	1030	S	38	SG27	1086	S	61	SG49	877	C
16	SG13	1063	S	39	SG28	833	C	62	SG50	1285	S
17	SG14	951	S	40	SG29	811	S	63	SG51	1033	S
18	SG15	935	C	41	SG30	1030	S	64	SG52	869	S
19	SG16	995	S	42	SG31	1081	S	65	SG52	883	S
20	SG17	1075	S	43	SG32	1132	S	66	SG52	882	S
21	SG18	859	S	44	SG33	943	S	67	SG52	883	S
22	SG18	879	S	45	SG34	1282	S	68	SG52	891	S
23	SG18	887	S	46	SG35	1231	S	69	SG53	1082	S

(a) C stands for clinopyroxene and S for spinel. The presence of RuO_2 was ignored.

The T_L for some glasses was measured more than once under different conditions to rule out different effects as indicated in Table II-S.

Table II-S. Repeated Measurements

	ID	*Comments*
3	SG02	cooled down from T > T_L, heat-treatment 70 h
7	SG06	suspect value, new measurement
8	SG06	original glass
9	SG06	glass with 0.03 wt% RuO_2, T_{M2} = 1222°C
21	SG18	suspect value, new measurement
23	SG18	using ASTM C-829 sample preparation procedure
24	SG18	using ASTM C-829 sample preparation procedure
27	SG18	using ASTM C-829 sample preparation procedure
35	SG25	original glass
36	SG25	glass with 0.03 wt% RuO2, T_{M2} = 1233°C
60	SG48	cooled down from T > T_L
64	SG52	suspect value, new measurement
66	SG52	using ASTM C-829 sample preparation procedure
68	SG52	using ASTM C-829 sample preparation procedure

All glasses formed an iron-containing primary phase: nine glasses formed an acmite-augite clinopyroxene phase; all other glasses formed spinel. These phases formed by bulk crystallization. Spinel nucleation was virtually instantaneous, and its growth rate was rapid. Occasionally, spinel nucleated on RuO_2 needle-like crystals that precipitated from the glass. Spinel contained Fe_2O_3, FeO, NiO, and Cr_2O_3 as major components; minor components were MnO, MgO, Al_2O_3, and (possibly) RuO_2.

The T_L values for the DWPF glasses ranged from 865°C to 1316°C for spinel and from 793°C to 996°C for clinopyroxene. The DWPF T_L database obtained for the spinel primary phase was checked against the following previously produced T_L databases: Hanford Phase 1 privatization data, Hanford spinel (SP) study, and uranium-effect scoping study data. The DWPF was compatible with these databases, based on as-batched glass compositions and partial specific liquidus temperatures for 14 glass components.

According to their effects on T_L, glass components fall into four groups:

$$(Cr_2O_3, NiO) >> (MgO, TiO_2, Al_2O_3, Fe_2O_3) >$$
$$(U_3O_8, MnO, CaO, B_2O_3, SiO_2) > (K_2O, Li_2O, Na_2O)$$

Oxides in the first group (Cr_2O_3, NiO, and possibly RuO_2) strongly increase T_L. Replacing 1 mass% SiO_2 by 1 mass% Cr_2O_3 increases T_L by 200°C to 300°C, and replacing 1 mass% SiO_2 by 1 mass% NiO increases T_L by 70°C to 90°C. Oxides in the second group (MgO, TiO_2, Al_2O_3, and Fe_2O_3) moderately increase T_L (by 15°C to 30°C). Oxides in the third group (U_3O_8, MnO, CaO, B_2O_3, and SiO_2) have little effect (they increase T_L by 0°C to 10°C). Alkali oxides (K_2O, Li_2O, and Na_2O) decrease T_L by 0 to 10°C. The validity of these estimates is restricted to the composition region of the test matrix.

The present study did not investigate the effect of glass redox. Assessing the effect of glass redox on T_L would reduce uncertainty in the T_L-composition relationship.

Waste-glass optimization for DWPF can be significantly enhanced using the T_L database presented in this report.

Acknowledgments

The authors appreciate the guidance and funding for this task provided by the U.S. Department of Energy Office of Science and Technology and the Tanks Focus Area.

This study is the result of an effort made by a large number of people, of whom only some can be mentioned. First of all, the authors are grateful to colleagues from the Savannah River Technology Center for their guidance and continuous interest in our work, namely, Bill Holtzscheiter (the Technical Integration Manger from the Tanks Focus Area), Bond Calloway, David Peeler, Carol Jantzen, and Kevin Brown. We also appreciate the interest and help from the Pacific Northwest National Laboratory Environmental Science and Technology Office, in particular from Bill Bonner, Charlotte Blair, and April Wagner.

We received significant technical support as well. Tommy Edwards from the Savannah River Technology Center developed the test matrix. Mike Schweiger, an experienced technical specialist, has trained and advised two of the authors (Martin Mika and Jarrod Crum) in their technical work. Ron Sanders and Meiling Gong chemically analyzed glasses and crystals. Adam Moule worked on the relationship between spinel composition and temperature. Jim Young performed scanning electron microscopy-energy dispersive x-ray spectrometry phase identification and analyses, and David MrCready conducted a part of the x-ray diffraction work. The authors also thank Wayne Cosby for editorial support.

Acronyms

ASTM	American Society for Testing and Materials
CVS	composition variation study
DWPF	Defense Waste Processing Facility
EDS	electron dispersive spectroscopy
EDXRF	energy dispersive x-ray fluorescence
FY	fiscal year
HLW	high-level waste
ICP-AES	inductively coupled plasma-atomic emission spectroscopy
ICP-MS	inductively coupled plasma-mass spectroscopy
LRB	laboratory record book
M&TE	measuring and test equipment
NBS	National Bureau of Standards[1]
PCT	product consistency test
PNNL	Pacific Northwest National Laboratory
SEM	scanning electron microscopy
SRS	Savannah River Site
SRTC	Savannah River Technology Center
TFA	Tanks Focus Area
TTP	technology task plan
XRD	x-ray diffraction

[1] Presently National Institute of Standards and Technology (NIST).

Contents

Tables

Figures

1.0 Introduction

The Defense Waste Processing Facility (DWPF) at the Savannah River Site (SRS) began radioactive operations on March 12, 1996 [1]. SRS currently plans to vitrify roughly 1.3×10^5 m^3 (and 5.0×10^8 Ci) of high-level waste (HLW) over the next several years to produce nearly 6,000 canisters of HLW glass [2] at an estimated cost of roughly \$1M per canister.[2] The volume of glass to be produced depends on the fraction of the mass of glass originating from the waste (the waste loading). A 1 mass% increase in DWPF glass waste loading could decrease the number of canisters by roughly 200, reducing cleanup costs by \$200M. Recent research at Pacific Northwest National Laboratory (PNNL)[3] has revealed a possibility of up to 20 mass% gain in the loading of HLW for Hanford's Phase I privatized vitrification.[4] This result was achieved because of a large database of glass compositions and properties accumulated over 8 years [4-16]. Efforts to increase waste loading by obtaining critical glass property data are now turned toward DWPF glass in this report—and Hanford Phase II privatization in a subsequent study.

Data from DWPF's first year of operation show that waste loading is limited by liquidus temperature (T_L) with spinel primary phase. Spinel forms in glasses with high concentrations of Cr, Ni, and/or Fe [14-17]. Spinel formation may have an adverse impact on both melter performance and processing. Spinel can cause sludge accumulation in the melter, pouring difficulties, cold-cap freezing, and foam stabilization. To avoid these problems, T_L is required to be lower than the lowest temperature of glass in the melter, which is estimated 100°C below the nominal melter operating temperature (1150°C).

---

[2] This is an estimate based on assumptions that are uncertain due to several unknown factors—compare Ref. [3].

[3] Pacific Northwest National Laboratory is operated for the U.S. Department of Energy by Battelle under Contract DE-AC06-76RLO 1830.

[4] J. D. Vienna, M. J. Schweiger, D. E. Smith, H. Li, and P. Hrma, "Phase I Privatization High-Level Waste Glass Data Support," Interim Data Package, Pacific Northwest National Laboratory, Richland, Washington, 1996. The nominal waste loading in Phase I privatization glasses calls for W' = 25 mass% of waste components other than SiO_2 and Na_2O. This translates to different levels of waste loading (W > W'), according to the SiO_2 and Na_2O content in the waste streams. For most waste streams, $W_{opt} > W$, where the optimized waste loading (W_{opt}) is up to 20 mass% higher than W.

Process-control models have been developed in DWPF that relate glass composition to several glass properties, including T_L. However, the DWPF T_L model uncertainty is considerable because the model is based on a limited number of T_L data [11, 18].[5] Producing additional data and reducing measurement and prediction errors will result in a less uncertain estimate of T_L and will thus allow increased waste loading in DWPF glass. Previous studies at PNNL resulted in developing T_L measurement techniques with reduced uncertainty. These techniques were used to determine compositional effects on the T_L of Hanford HLW glasses [8,14-17,19].

Staff at the Savannah River Technology Center (SRTC) reviewed different T_L measurement techniques to identify an appropriate method for DWPF model enhancement [20]. They concluded that the uniform temperature measurement procedure proposed by PNNL to the American Society for Testing Materials (ASTM)[6] and a procedure currently being developed at SRTC were appropriate for the T_L measurement of DWPF glasses tested in this study.

This report provides new T_L versus composition data that can be used to reduce uncertainty in T_L calculation for DWPF glass. According to the test plan[7] and test matrix design,[8] PNNL has measured T_L for 53 glasses within and just outside of the current DWPF processing composition window. The T_L database generated under this task will directly support developing and enhancing the current T_L process-control model. Preliminary calculations have shown a high probability of increasing HLW loading in glass produced at the SRS and Hanford. This increase in waste loading will decrease the lifecycle tank cleanup costs by decreasing process time and the volume of waste glass produced.

---

[5] The DWPF T_L database is restricted to glasses that melt at 1150°C.

[6] J. D. Vienna, P. Hrma, M. J. Schweiger, and D. E. Smith, "Standard Test Methods for Determining the Liquidus Temperature (T_L) of Waste Glasses," Submitted to the ASTM C26 Committee (1996).

[7] P. Hrma and J. D. Vienna, "Optimization of Waste Loading in Glass, Test Plan for Spinel Study," Pacific Northwest National Laboratory, Richland, Washington, 1997.

[8] T. B. Edwards, "A Statistically Designed Sampling Plan for Investigating Liquidus Temperature Versus Glass Composition (U)," Inter-Office Memorandum, SRT-SCS-97-0022, Westinghouse Savannah River Company, Aiken, South Carolina, 1997.

2.0 Objective

The main objective of this work is to increase the waste loading in HLW glasses produced at SRS and Hanford by developing a database for glass composition effects on T_L because T_L limits waste loading in current glass formulations (see the Technology Task Plan[9]).

[9] Technology Task Plan (TTP), RL3-7-WT-31, Pacific Northwest National Laboratory, Richland, Washington, 1997.

3.0 Experimental

This section describes the experimental design (Section 3.1), glass preparation (Section 3.2), and the T_L measurement method (Section 3.3.6). The goal of the experimental design is to generate a DWPF T_L database that can be used to develop improved T_L-composition relationships with less uncertainty. The waste loading of DWPF HLW glass and most of Hanford HLW glasses is limited by glass crystallization. Hence, T_L directly impacts estimates of the optimal waste loading. The test matrix was designed by SRTC to develop a database for waste loading optimization that can adequately support developing an improved T_L–composition relationship for use in DWPF process-control schemes.

3.1 Experimental Design

The composition region of the DWPF-relevant test matrix[10] (denoted as SG series of glasses) was based on the DWPF glass composition region. These two composition regions and the preliminary composition region of HLW glass for Hanford wastes prone to spinel crystallization (denoted as the SP series [15]) are shown in Table 3.1.

Table 3.2 lists the 51 unique SG glasses, which comprise a layered statistical design[11] produced at SRTC by T. B. Edwards.[12] The layered design consists of 36 compositions on the boundary, 14 compositions on an interior layer, and one center composition of the SG composition region. Two duplicates, one of the centroid glass (SG05) and one of an extreme vertex (SG 18), extend the number of test glasses to 53. This test matrix contains glass compositions within and just outside the DWPF composition region. This study is currently being expanded to include the composition region for Hanford HLW glass (which is larger than the DWPF region).

---

[10] See Footnote 8.

[11] G. F. Piepel, C. M. Anderson, and P. E. Redgate, "Response Surface Designs for Irregularly-Shaped Regions" (Parts 1, 2, and 3), *1993 Proceedings of the Section on Physical and Engineering Sciences*, 205-227, American Statistical Association, Alexandria, Virginia, 1993.

[12] See Footnote 8.

Table 3.1. Composition Regions for DWPF, SG, and SP Glasses (in Mass Fractions of Components)

	DWPF Region		SG Glasses		SP Glasses	
Oxide[a]	Low	High	Low	High	Low	High
SiO_2	.491	.551	.430	.590	.380	.600
B_2O_3	.068	.075	.050	.100	.000	.120
Al_2O_3	.024	.055	.025	.080	.040	.160
Li_2O	.043	.050	.030	.060	.000	.030
Na_2O	.078	.106	.060	.110	.080	.200
K_2O	.021	.026	.015	.038	.000	.000
MgO	.013	.021	.005	.025	.004	.060
CaO	.007	.013	.003	.020	.000	.000
MnO	.011	.028	.010	.030	.000	.040
NiO	.001	.012	.001	.020	.000	.030
Fe_2O_3	.085	.124	.060	.150	.060	.150
Cr_2O_3	.000	.002	.001	.003	.000	.012
TiO_2	.002	.004	.002	.006	.000	.000
U_3O_8	.008	.050	.000	.055	.000	.000
Others[b]			.000	.000	.045	.070

(a) SG glasses contained RuO_2 in mass fraction 0.0009. SP glasses contained RuO_2 in mass fraction 0.0003. The estimated RuO_2 mass fraction for the DWPF composition region is 1×10^{-5} to 0.0015.

(b) Others for SP glasses were a mixture of 22 minor components with ZrO_2, Nd_2O_3, La_2O_3, CdO, MoO_3, F, and SO_3 > 3 mass% of the mix.

3.2 Glass Fabrication

We used laboratory practices established at PNNL to prepare glass and measure T_L. All laboratory data, general observations, and details of the activities performed in this study are recorded in Laboratory Record Book (LRB) # BNW56241. Subsequent notebooks are cross-referenced. All instrument calibrations and materials are traceable to test samples. The identity, including calibration category, status, and number, of all measuring and test equipment (M&TE)

used for this study are recorded in the LRB. The M&TE includes balances, thermocouples, and temperature displays. Chemicals used to prepare glass were of reagent grade, and their sources are recorded in the LRB.

3.2.1 Batching and Melting Glasses

Batches were prepared to make 450 g of glass. This amount was sufficient to measure T_L, analyze the glass, and archive samples for future characterization (viscosity, chemical durability, and phase homogeneity testing). Glasses were made according to PNNL procedure, PSL-417-GBM, "Procedure for Glass Batching and Melting." Batch chemicals [oxides, alkali and calcium carbonates, boric acid, and $Ru(NO)(NO_3)_3$] were mixed in an agate milling chamber for 6 min and melted for 1 h in a Pt-10%-Rh crucible covered with a platinum lid in a Deltech Dt-31 furnace.

The first nonradioactive glass, SG02, was prepared by melting the batch at 1150°C for 1 h, followed by milling and remelting under the same conditions. A thin section prepared from this glass showed a large number of undissolved RuO_2 agglomerates that interfered with the detection of spinel crystals. To reduce undissolved RuO_2, the melting temperature of SG02 glass was increased to 1250°C for 2 h. As a result, the occurrence of undissolved RuO_2 particles in the glass decreased, partly by further agglomeration, partly by dissolution, and possibly by volatilization[13] (see Sections 3.3.1 and 6.2.6). Thin sections of this glass could be used for a reliable detection of spinel crystals. Based on this result, we melted each SG glass at the temperature $T_{M1} \geq T_5 + \Delta T$, where T_5 is the temperature at which the calculated melt viscosity was 5 Pa·s and ΔT was approximately 100°C.[14] The T_5 value was estimated from Hanford viscosity database [14], which is broader than the composition region of SG glasses. The partial specific Vogel-Fulcher-Tammann viscosity coefficients [14b] are listed in Table 3.3.

---

[13] Volatilization of RuO_2 particles was unlikely because these particles were embedded in the glass.

[14] Both T_{M1} and T_5 for each SG glass are listed in Section 4.1 (Table IV).

Table 3.2. Glass Compositions (in Mass Fractions) for the DWPF Region[a]

ID	[b]	Al_2O_3	B_2O_3	CaO	Cr_2O_3	Fe_2O_3	K_2O	Li_2O	MgO	MnO	Na_2O	NiO	SiO_2	TiO_2	U_3O_8
SG01	E	.0250	.0999	.0200	.0010	.1499	.0380	.0599	.0050	.0100	.0599	.0200	.4496	.0060	.0550
SG02	E	.0250	.0500	.0200	.0010	.0599	.0380	.0599	.0250	.0300	.1099	.0005	.5785	.0015	.0000
SG03	I	.0390	.0876	.0158	.0025	.1202	.0208	.0375	.0200	.0250	.0976	.0151	.4741	.0026	.0415
SG04	E	.0799	.0500	.0030	.0010	.1499	.0150	.0599	.0250	.0100	.0599	.0200	.5240	.0015	.0000
SG05	C	.0530	.0752	.0115	.0020	.1052	.0266	.0450	.0150	.0200	.0852	.0102	.5276	.0037	.0280
SG06	E	.0799	.0500	.0200	.0010	.1499	.0380	.0300	.0050	.0100	.1099	.0005	.4991	.0060	.0000
SG07	E	.0799	.0999	.0030	.0030	.0599	.0380	.0599	.0250	.0300	.0599	.0005	.5385	.0015	.0000
SG08	I	.0390	.0626	.0158	.0015	.1275	.0323	.0375	.0200	.0250	.0726	.0054	.5397	.0026	.0177
SG09	E	.0799	.0999	.0200	.0030	.1499	.0150	.0599	.0050	.0100	.0599	.0005	.4396	.0015	.0550
SG10	I	.0390	.0626	.0073	.0025	.0825	.0323	.0525	.0200	.0250	.0726	.0151	.5437	.0026	.0415
SG11	I	.0390	.0876	.0073	.0015	.0825	.0208	.0525	.0200	.0150	.0976	.0054	.5497	.0026	.0177
SG12	E	.0250	.0500	.0030	.0030	.1499	.0150	.0300	.0250	.0100	.1099	.0005	.5765	.0015	.0000
SG13	E	.0250	.0999	.0030	.0030	.0874	.0150	.0599	.0050	.0300	.0599	.0200	.5895	.0015	.0000
SG14	E	.0250	.0999	.0030	.0010	.1499	.0380	.0300	.0250	.0300	.1099	.0005	.4306	.0015	.0550
SG15	E	.0250	.0999	.0200	.0010	.0599	.0150	.0599	.0250	.0100	.0599	.0200	.5895	.0060	.0080
SG16	I	.0664	.0626	.0158	.0015	.0825	.0208	.0525	.0200	.0250	.0976	.0054	.5026	.0049	.0415
SG17	I	.0390	.0725	.0158	.0015	.1275	.0323	.0525	.0100	.0150	.0976	.0151	.4741	.0049	.0415
SG18	E	.0250	.0999	.0030	.0030	.1499	.0150	.0599	.0050	.0300	.1099	.0005	.4921	.0060	.0000
SG19	E	.0799	.0999	.0030	.0030	.0599	.0380	.0599	.0050	.0100	.1099	.0200	.4541	.0015	.0550
SG20	E	.0799	.0500	.0200	.0010	.0599	.0150	.0599	.0250	.0100	.1099	.0005	.5070	.0060	.0550

ID	[b]	Al_2O_3	B_2O_3	CaO	Cr_2O_3	Fe_2O_3	K_2O	Li_2O	MgO	MnO	Na_2O	NiO	SiO_2	TiO_2	U_3O_8
SG21	I	.0390	.0876	.0158	.0025	.0825	.0208	.0525	.0100	.0242	.0726	.0151	.5540	.0049	.0177
SG22	I	.0664	.0626	.0158	.0025	.1275	.0208	.0525	.0100	.0150	.0976	.0151	.4931	.0026	.0177
SG23	I	.0417	.0626	.0158	.0025	.0825	.0323	.0375	.0200	.0150	.0976	.0151	.5540	.0049	.0177
SG24	E	.0250	.0500	.0030	.0010	.1194	.0150	.0599	.0050	.0100	.0599	.0005	.5895	.0060	.0550
SG25	E	.0799	.0999	.0030	.0010	.1499	.0380	.0300	.0250	.0100	.0599	.0200	.4811	.0015	.0000
SG26	I	.0390	.0626	.0073	.0025	.1275	.0208	.0375	.0100	.0150	.0976	.0054	.5276	.0049	.0415
SG27	I	.0664	.0876	.0158	.0025	.1109	.0323	.0525	.0200	.0150	.0726	.0054	.4741	.0026	.0415
SG28	E	.0250	.0999	.0200	.0010	.1499	.0150	.0599	.0050	.0100	.1099	.0005	.5015	.0015	.0000
SG29	E	.0799	.0500	.0030	.0010	.0599	.0150	.0599	.0050	.0300	.1099	.0005	.5240	.0060	.0550
SG30	E	.0799	.0500	.0200	.0010	.0599	.0380	.0599	.0250	.0300	.1099	.0200	.4491	.0015	.0550
SG31	E	.0799	.0999	.0200	.0010	.1494	.0380	.0599	.0250	.0300	.0599	.0005	.4296	.0060	.0000
SG32	E	.0799	.0999	.0030	.0010	.1499	.0150	.0599	.0050	.0100	.1099	.0200	.4396	.0060	.0000
SG33	E	.0799	.0999	.0200	.0030	.0599	.0380	.0599	.0050	.0300	.1099	.0200	.4676	.0060	.0000
SG34	E	.0799	.0999	.0200	.0030	.1454	.0150	.0300	.0250	.0300	.0599	.0005	.4296	.0060	.0550
SG35	E	.0799	.0500	.0030	.0030	.1449	.0380	.0599	.0250	.0300	.1099	.0200	.4296	.0060	.0000
SG36	E	.0250	.0999	.0200	.0030	.0599	.0380	.0300	.0050	.0100	.1099	.0005	.5415	.0015	.0550
SG37	E	.0250	.0999	.0200	.0030	.0599	.0380	.0599	.0250	.0100	.0599	.0030	.5895	.0060	.0000
SG38	E	.0250	.0999	.0030	.0010	.1464	.0380	.0300	.0250	.0300	.1099	.0005	.4296	.0060	.0550
SG39	E	.0250	.0500	.0200	.0030	.1499	.0150	.0300	.0050	.0300	.1099	.0200	.5355	.0060	.0000
SG40	E	.0799	.0999	.0030	.0030	.0599	.0150	.0300	.0250	.0100	.1099	.0200	.4826	.0060	.0550
SG41	E	.0799	.0999	.0200	.0010	.1499	.0150	.0300	.0050	.0300	.0599	.0200	.4321	.0015	.0550
SG42	I	.0449	.0876	.0073	.0025	.1275	.0323	.0525	.0200	.0250	.0976	.0054	.4741	.0049	.0177
SG43	I	.0664	.0876	.0073	.0015	.0825	.0323	.0375	.0100	.0250	.0976	.0054	.5257	.0026	.0177

ID	(b)	Al_2O_3	B_2O_3	CaO	Cr_2O_3	Fe_2O_3	K_2O	Li_2O	MgO	MnO	Na_2O	NiO	SiO_2	TiO_2	U_3O_8
SG44	I	.0664	.0876	.0073	.0015	.1275	.0208	.0375	.0200	.0150	.0726	.0151	.5052	.0049	.0177
SG45	E	.0250	.0999	.0200	.0010	.0599	.0150	.0300	.0250	.0300	.1099	.0200	.5620	.0015	.0000
SG46	E	.0250	.0500	.0030	.0030	.1499	.0380	.0599	.0250	.0100	.0599	.0200	.4946	.0060	.0550
SG47	E	.0250	.0500	.0200	.0030	.1499	.0150	.0599	.0250	.0100	.1099	.0200	.4551	.0015	.0550
SG48	E	.0270	.0999	.0030	.0010	.0599	.0380	.0300	.0050	.0100	.1099	.0200	.5895	.0060	.0000
SG49	E	.0250	.0500	.0030	.0010	.0809	.0380	.0599	.0050	.0300	.0599	.0005	.5895	.0015	.0550
SG50	E	.0250	.0500	.0200	.0030	.1499	.0380	.0300	.0050	.0300	.0599	.0200	.5075	.0060	.0550
SG51	E	.0799	.0500	.0200	.0030	.1499	.0380	.0300	.0050	.0100	.1099	.0005	.5015	.0015	.0000
SG52	D	.0250	.0999	.0030	.0030	.1499	.0150	.0599	.0050	.0300	.1099	.0005	.4921	.0060	.0000
SG53	D	.0530	.0752	.0115	.0020	.1052	.0266	.0450	.0150	.0200	.0852	.0102	.5276	.0037	.0280

(a) Oxides in the table sum to 0.9991; the remainder (0.0009) is RuO_2.

(b) C stands for the centroid, I for an internal point, and E for an extreme vertex.

Table 3.3. Partial Specific Vogel-Fulcher-Tammann Viscosity Coefficients [14][(a) (b)]

Oxide	A_i[(c)]	B_i, 10^3K	T_{0i}, K
Al_2O_3	-10.1	23.4	-338
B_2O_3	-1.7	-8.5	1283
CaO	-4.7	-10.3	1611
Fe_2O_3	-8.7	9	219
Li_2O	-16.3	-5.9	-460
MgO	-15.2	11.3	334
$Na_2O + K_2O$[(d)]	-7.1	-2.9	627
SiO_2	-2.9	9.6	656
Others[(e)]	-8.2	6.1	544

(a) Vogel-Fulcher-Tammann equation for viscosity is

$$\ln \eta = A + B/(T-T_0) \qquad \text{(I-1)}$$

where η is the viscosity, T is the absolute temperature, and A, B, and T_0 are composition-dependent coefficients.

(b) Partial specific values (glass properties, viscosity coefficients, etc.) are linear approximations defined by the equation

$$P = \sum_{i=1}^{N} P_i g_i \qquad \text{(I-2)}$$

where P is the property, P_i is the i-th component partial specific property, and g_i is the i-th component mass fraction in glass.

(c) $A = \ln \eta_0$, where η_0 is in Pa·s.

(d) The coefficients obtained in [14b] for Na_2O were applied to $Na_2O + K_2O$.

(e) Others are a mixture of Cr_2O_3, MnO, NiO, TiO_2, and U_3O_8. Others composition from [14b] is different. However, its effect on viscosity is negligible.

The glass was quenched by pouring it on a stainless steel plate and allowing it to cool to room temperature. Glass fibers were drawn from the melt and searched with an optical microscope for solid inclusions other than RuO_2. Glasses were then milled in a tungsten carbide chamber for 8 min and remelted for 1 h. If large amounts of undissolved RuO_2 or large spinel

crystals (2 to 3 μm or larger, indicating that $T_{M1} < T_L$) were present, the glass was remelted at a higher temperature. Otherwise, the temperature of the second melt was the same as that of the initial melt. Only SG02 glass was melted three times as described above. The final melting temperature (T_{M2}) is shown for each glass in Section 4.1 (Table 4.1). Glass was quenched on a stainless steel plate and crushed in a plastic bag.[15]

3.2.2 Glass Analysis

We sent all glasses to SRTC for chemical analysis. The results will be reported separately. However, the composition of SG06 glass was checked at PNNL to assess the impact of volatilization. SG06 was chemically analyzed with inductively coupled plasma-atomic emission spectroscopy and mass spectrometry (ICP-AES and ICP-MS). In the ICP measurement, the glass was fused in Na_2O_2 and KOH according to the standard procedures, ASTM C1317-95, "Practice for Dissolution of Silicate or Acid Resistant Matrix Samples" and PNL-ALO-235, "Sample Preparation of Rocks, Glasses, and Sediments by Sodium Peroxide and Lithium Metaborate Fusion." The results are shown in Section 6.2.4.

3.3 Liquidus Temperature Measurement

Liquidus temperature is the highest temperature at which melt and the primary crystalline phase can coexist at equilibrium. At $T > T_L$, the only equilibrium phase is the melt without crystals. We considered several factors that might affect the capability to obtain a repeatable T_L measurement: 1) presence of RuO_2, 2) crystallization or dissolution rate of the primary phase, 3) volatilization of alkalis and alkali borates, 4) redox equilibrium with the atmosphere, and 5) crystallization during quenching. These issues are discussed in Sections 3.3.1 to 3.3.5. The T_L measurement method is described in Section 3.3.6.

---

[15] The ASTM C 829-81 (reapproved 1995) procedure requires that pieces of quenched glass are washed with acetone, rinsed with deionized water, dried, crushed using mortar and pestle, passed through a 850-μm sieve, and treated with a magnet. At SRTC request, samples of glasses SP-1 and SG18 were prepared following this procedure. Two samples from each glass, one prepared by the ASTM procedure and the other by the direct heat-treatment of crushed glass, were placed into two separate crucibles and heat-treated simultaneously in the same furnace. The T_L - $T_{L,ASTM}$ difference was 0°C for SP-1 glass and –8°C for SG18 glass. This difference is within the experimental error.

3.3.1 Presence of RuO_2

As described in Section 3.2.1, glasses were melted at temperatures high enough to avoid excessive concentration of undissolved RuO_2 that would otherwise prevent accurately determining T_L. A part of the dissolved RuO_2 precipitated on subsequent cooling in the form of needle-like crystals in some glasses. Agglomerates of undissolved RuO_2 and needle-like crystals of precipitated RuO_2 are shown in Figure 3.1. The needle-like RuO_2 crystals did not interfere with spinel identification. RuO_2 did not interfere with the detection of clinopyroxene because the large distinctive crystals of this phase were easy to notice.

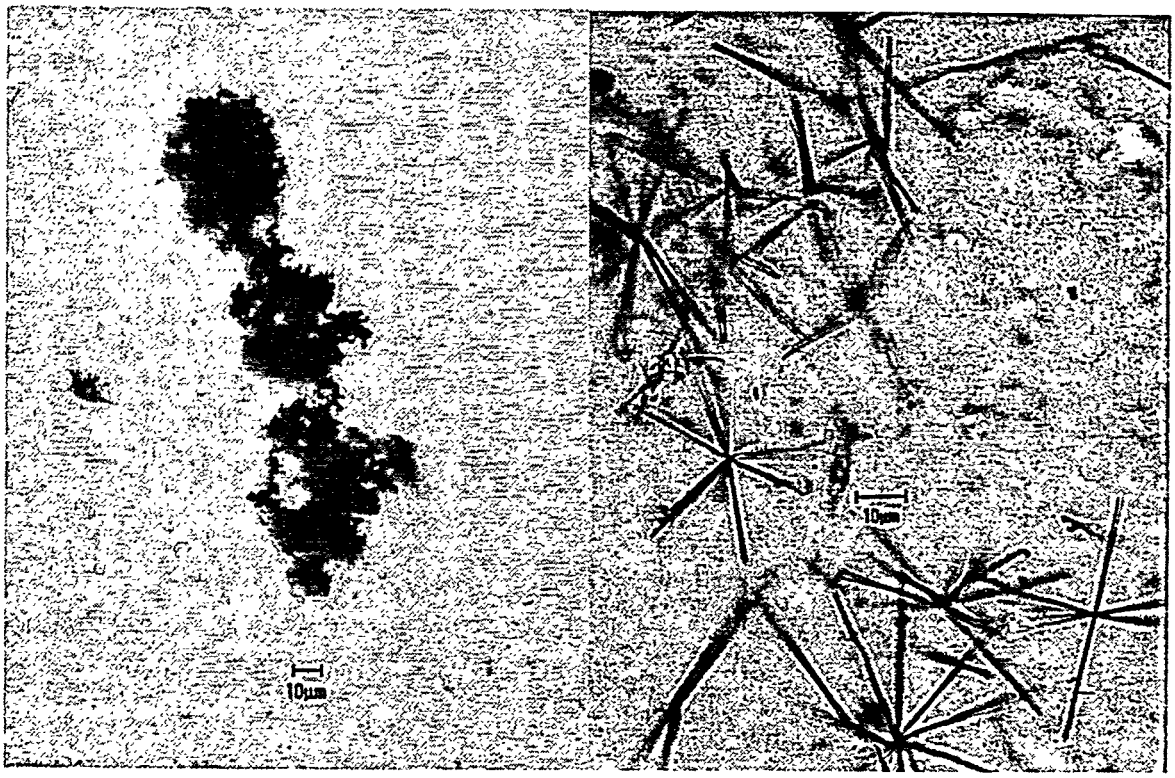

(a) (b)

Figure 3.1. Optical Micrographs of RuO_2 Agglomerates (a) and Needle-like Crystals (b)

3.3.2 Crystallization/Dissolution Rate of Spinel

According to a spinel crystallization kinetics study [17], spinel crystallization can be described by the Avrami equation

$$\frac{C}{C_{eq}} = 1 - \exp\left\{1 - \left[\left(\frac{t}{\tau_0}\right)\exp\left(-\frac{B_\tau}{T}\right)\right]^{1.5}\right\} \quad (1)$$

where C is the spinel volume fraction in glass at time t, C_{eq} is the equilibrium spinel volume fraction in glass, and T is the absolute temperature. For a typical borosilicate HLW glass [17], $\tau_0 = 0.006311$ s and $B_\tau = 14250$ K. With these values, the time to reach $C = 0.95C_{eq}$ is 128 min at 800°C, 41 min at 900°C, 16 min at 1000°C, and 7 min at 1100°C. Spinel nucleation being virtually instantaneous, these times provide an estimate for the heat-treatment time to bring glass samples to a reasonable proximity of phase equilibrium. The actual heat-treatment times were 1 to 2 orders of magnitude longer (Section 3.3.6).

Crystals generally dissolve slower than they form, especially when crystals agglomerate. Dissolving crystals can easily be recognized by rounded edges. These crystals appeared occasionally at $T > T_L$ at short heat-treatment times. As glass samples approached redox equilibrium with atmospheric air, these crystals dissolved (Section 3.3.4).

3.3.3 Volatilization of Alkalis and Alkali Borates

Previous studies [14] have shown that volatilization does not measurably affect the composition of 0.5-kg glass batches during melting under a lid (Sections 3.2.1 and 6.2.4). However, small glass samples used for heat-treatment could be affected by evaporation from the meniscus area [21,22]. Glass depleted of alkalis has a higher T_L [15,16]. In a temperature gradient method, samples placed in a boat are affected at $T > 850$°C because of crystals drifting towards the hot end of the boat—see Section 6.2.5—even at a very mild temperature gradient of 1°C/mm. In the uniform temperature method used in this study, volatilization affects small glass samples at $T > 1200$°C. To minimize volatilization, we shortened the heat-treatment of glass with $T_L > 1200$°C to 1 to 3 h. This time was still several times longer than the estimated time needed for establishing phase equilibrium and was sufficient for establishing redox equilibrium (see the following section). However, at $T < 1200$°C, when volatilization is less severe, a longer heat-treatment time was used to ensure redox equilibrium with the atmosphere.

3.3.4 Redox Equilibrium with the Atmosphere

Melting the glass at an elevated temperature to reduce the number of undissolved RuO_2 particles (Section 3.2.1) resulted in a higher redox ratio of iron (Fe^{2+}/Fe)—see Section 6.2.7.

Glasses reach a higher redox ratio rapidly by generating oxygen bubbles. However, reoxidation at a lower temperature is a slow process controlled by diffusion from the surrounding atmosphere. To obtain reproducible and well-defined T_L data, samples were heat-treated for a time sufficient to reach redox equilibrium with air (Section 3.2.2). This time is a function of temperature. The approach to redox equilibrium could be observed in thin sections from the changing color of some samples, from greenish to brown-yellow. Crystals that initially precipitated from a reduced sample eventually redissolved as the sample approached redox equilibrium.

3.3.5 Crystallization During Quenching

All glasses were melted at $T > T_L$. No crystals other than undissolved RuO_2 were seen in fibers pulled from the glass during the second melt at the final melting temperature T_{M2}. While the glass was quenched in air to room temperature, tiny spinel crystals (< 1 μm) formed within some samples. These crystals rapidly dissolved at $T > T_L$. Tiny spinel crystals could reappear while the samples were quenched in air after the heat-treatment. For glasses with $T_L \leq 1200°C$, these secondary crystals were barely visible by an optical microscope (they appeared as tiny dust) and thus were easily distinguishable from the larger crystals (≥4 μm) that grew during the heat-treatment. For glasses with $T_L > 1200°C$, the secondary crystals were larger (about 1 μm). To ensure that these crystals were not interfering with T_L measurement, glasses with $T_L >$ 1200°C were quenched in water. Water-quenched samples were cooled rapidly enough that secondary crystals did not form. Quenching in water caused cracking and was not used for glasses with T_L <1200°C.

3.3.6 T_L Measurement Technique

T_L was measured using uniform temperature furnaces following PNNL procedure GDL-LQT "Liquidus Temperature Measurement Procedure." Approximately 2.5 g of glass was placed into square Pt-10%-Rh containers with lids and heat-treated at constant temperature[16] in a

---

[16] The sample can be heated up or cooled down to the heat-treatment temperature. The heat-up method was used in this study. The cool-down method was not used for several reasons. First, melting small samples at $T > T_L$ may cause severe volatilization. Second, molten samples tend to lose melt by capillary elevation and drainage between the platinum crucible and lid. Third, melting the glass destroys nuclei and thus may prevent crystallization near T_L, especially for clinopyroxene with its long incubation time (approximately 10 h near T_L [31]). At SRTC request, glasses SG02 and SG48, both of which precipitate clinopyroxene—see Table 3.4—were first heat-treated at $T > T_L$

Deltech-31 furnace for a standard time of 22 h. Exceptionally, samples with $T_L < 1200°C$ were heat-treated for $t < 22$ h (down to 13 h) at $T < T_L$. A heat-treatment time > 22 h (up to 65 h) was occasionally used to ensure that redox equilibrium was reached. Samples with $T_L > 1200°C$ were treated for 1 to 3 h (1 h was sufficient for redox equilibrium at $T > 1200°C$) to reduce volatilization.

Samples were quenched in air except 9 glasses (SG04, 25, 32, 34, 35, 41, 44, 46, and 50) with $T_L > 1200°C$, which were quenched in water to reduce massive secondary crystallization that caused opaqueness of glass. Nonradioactive samples were thin-sectioned, polished, and examined by optical microscopy (Olympus PMG 3) using transmitted light. For radioactive samples, glass was placed into a plastic bag, broken with a hammer, and 10 to 20 thin chips (1 to 3 mm in size) were glued to a microslide and examined. This number and size of chips were sufficient to obtain a representative sample for crystal detection near T_L. The total volume of chips was equal to or larger than the volume of a thin section (approximately 20 mL). Although spinel tends to be distributed nonuniformly in glass, and its crystals are sparse near T_L, 1 to 3 mm samples were large enough to eliminate any bias with respect to thin-sectioned samples.

The heat-treatment of samples was repeated at successive temperatures above and below T_L until the difference in temperature between heat-treated glass samples with crystals (T_C) and without crystals (T_A) was narrowed down to ≤10°C. Six to ten heat-treatments per glass were usually needed. More than 400 heat-treatments were necessary for the 53 SG glasses. The difference between the measuring thermocouple and the sample temperature was assessed using the SP-1 glass,[17] PNNL internal standard, with $T_L = 1040°C$.[18].

(1000°C and 1100°C, respectively) for 1 h and then cooled in the same furnace to measure T_L. Clinopyroxene crystals were detectable in SG48 glass 15°C below T_L obtained by the heat-up method, which is a reasonable agreement considering the 10°C experimental error. No such agreement was achieved with glass SG02. When heat-treated for 24 h, glass SG02 produced no crystals down to 52°C below T_L. Li_2SiO_3 precipitated as the primary phase at 723°C and clinopyroxen as the secondary phase at $T \leq 718°C$. A long heat-treatment of 70 h was needed to produce clinopyroxene at 755°C.

[17] SP-1 glass composition in mass fractions: 0.0800 Al_2O_3, 0.0700 B_2O_3, 0.0022 Cr_2O_3, 0.1250 Fe_2O_3, 0.0300 Li_2O, 0.0060 MgO, 0.0036 MnO, 0.1573 Na_2O, 0.0052 NiO, 0.4600 SiO_2, and 0.0607 others (around 20 minor components).

The T_L value was determined from the presence or absence of crystals within the melt bulk. The bulk was considered the part of the sample at least 0.5 mm distant from the melt top, crucible walls, and crucible bottom. Near T_L, spinel crystals were located mostly within the bulk, except when some crystals sank to the bottom because of the density difference between spinel and glass. This happened when glass viscosity was low at T_L.

The T_L value within each ≤10°C interval was estimated according to the size, shape, and number of spinel crystals in the sample and is believed to be within ±5°C. However, the error in this T_L can be as high as ±10°C, considering the uncertainty in temperature measurement (Section 6.2.3), which is ±5°C by calibrated thermocouples. Two additional sources of error can be considered. First, the measured T_L value could be affected by the uncertainty in obtaining redox equilibrium with air at T_L. This uncertainty is unknown. No attempt was made to determine the redox of the samples after the heat treatment. The measurement of the redox effect on T_L will be done in FY 1999. Second, though the concentration of RuO_2 was constant throughout the SG test glasses, its actual concentration in the solution was not. Despite the elevated melting temperature, some RuO_2 remained undissolved within the glass and some dissolved RuO_2 precipitated. Thus uncertainty exists with respect to the effect of the dissolved RuO_2 on T_L. The effect of RuO_2 on T_L is being measured in FY 1999.

Crystalline phases in some samples were identified by X-ray diffraction (XRD) and scanning electron microscopy (SEM). All glasses were archived for future testing.

3.3.7 Furnace Calibration

Five furnaces were used to complete the large number of heat treatments within the tight schedule for this study. Subsequent testing showed that the heat-transfer conditions were different in each furnace, causing differences in temperature between the measuring thermocouple and the sample. The procedure used to assess (and ultimately adjust for) the temperature differences involved the following steps:

1. Measure the T_L of the NBS773 glass in each of the five furnaces.

---

[18] The T_L value reported in [15] was 1039°C. It was corrected to 1040°C, based on NBS773 standard glass. T_L was also measured on an SP-1 glass sample prepared using the ASTM procedure (see Footnote 14). The result was identical (T_L = 1040°C).

2. Measure the T_L of the SP-1 glass in each of the five furnaces.
3. Calculate a temperature difference for each furnace by subtracting the nominal T_L value (1040°C) of the SP-1 glass from the measured SP-1 T_L value for that furnace.
4. Adjust the T_L, T_C, and T_A values for the SG glasses (SG1 to SG53).
5. Apply the same temperature adjustments to the NBS773 measured T_L values for each furnace.
6. Assess the closeness of the NBS773 adjusted T_L values to the nominal value of 991°C ± 5°C.

Accordingly, the adjusted T_L values were $T_L = T'_L + \Delta T$, where T'_L is the unadjusted value and ΔT is the correction obtained as $\Delta T = T'_L(SP1) - 1140°C$. Temperature corrections across the five furnaces ranged from 1 to 33°C (ΔT = 1°C for Furnace 1, 20°C for Furnace 4, 33°C for Furnace 5, 6°C for Furnace 8, and 18°C for Furnace 9). Subsequent testing and modification of the furnaces following the move to a new laboratory confirmed that such large differences could exist. These differences are difficult to explain considering the extremely complex mechanism of heat transfer within a furnace. Presently, we reduce the magnitude of these differences by changing the positions of the sample and the thermocouple inside the furnace until the minimum temperature difference is obtained.

The unadjusted NBS773 T_L measurements in the five furnaces ranged from 995 to 1018°C, all of which are above the nominal value of 991°C. The adjusted NBS773 T_L measurements in the five furnaces ranged from 985 to 997°C (994°C in Furnace 1, 991°C in Furnace 4, 985°C in Furnace 5, 997°C in F urnace 8, and 988°C in Furnace 9), with a mean of 991.0°C and a standard deviation of 4.7°C. Hence, the adjusted values and their summary statistics compare very favorably with the nominal value and its uncertainty range of 991°C ± 5°C. This suggests that the adjustment process was successful in correcting for temperature differences in the furnaces.

Ideally, the T_L of the standard glasses should have been measured in each furnace before, several times during, and after making T_L measurements on the SG glasses. Then, the measured T_L values of the standard glasses (and their averages and standard deviations) could have been compared to the nominal values to statistically assess the presence or absence of a bias (constant or trend) for each furnace. Statistically significant biases could then have been corrected based

on such data. This ideal practice did not occur because of schedule and budget constraints for the work and the assumption that thermocouples placed very close to samples would give accurate temperatures (to within the calibration of the thermocouples). Still, the above six-step procedure (although not ideal) did allow for successfully assessing and adjusting for different temperature biases from furnace-to-furnace.

4.0 Results

Section 4.1 presents liquidus temperature values for SG glasses. Chemical analyses of crystals are reported in Section 4.2.

4.1 Liquidus Temperature

Table 4.1 shows the adjusted T_L values[19] (bold). Table 4.1 also shows the temperatures that characterize glass preparation and sample heat-treatment. T_5 is the temperature at which the glass viscosity was calculated [by Equation (I-1) under Table 3.3] to be 5 Pa·s. T_{M1} and T_{M2} are the melting temperatures of the first and second (third in the case of SG02) melting. T_C stands for the highest heat-treatment temperature at which a crystalline phase was found, and T_A stands for the lowest temperature at which the sample was amorphous after heat-treatment (hence, $T_A \geq T_L \geq T_C$). Table 4.1 also indicates the primary phase and the presence of RuO_2 needle-like crystals (see Figure 3.1b). Ignoring the presence of RuO_2 crystals, the primary crystallization phase was spinel in all but 7 glasses (SG02, 15, 24, 28, 36, 48, and 49), in which the primary phase was clinopyroxene. In glasses SG20 and SG45, both spinel and clinopyroxene were found to form between T_C and T_A. Clinopyroxene crystals are displayed in Figure 4.1.

The T_L values for the DWPF SG glasses range from 865°C to 1316°C for spinel as the primary phase and from 793°C to 996°C for clinopyroxene as the primary phase. The number of glasses for which $T_L < 1050$°C is 28, of which 26 have predicted viscosity 5 Pa·s between 1040°C and 1250°C.

The size of spinel crystals was typically 4 to 12 μm, although crystals as small as 1 μm could form during heat-treatment. Crystals formed during heat-treatment were generally distinguishable from much smaller crystals (<1 μm) that precipitated during quenching (see Section 3.3.5). Spinel crystals occurred in three different forms. Spinel cubes were most common. In some glasses (SG04, 41, and 46), the edges and corners grew more rapidly than the walls, creating star-shaped crystals (Figure 4.2). Both cubes and stars were present in SG04 glass. In SG11, 13, 20, 21, and 44 glasses, spinel crystals grew on RuO_2 needles.

---

[19] Henceforth, references to T_L values for the SG glasses should be assumed to be "adjusted" values as described in Section 3.3.7.

Table 4.1. Melting and Liquidus Temperatures (in °C) of Test Glasses

Glass[a]	T_5[e]	T_{M1}[f]	T_{M2}[f]	T_L[b]	T_C[g]	T_A[h]	PP[c]
SG01	1007	1107	1107	**1124**	1119	1130	S
SG02[d]	1129	1150	1250	**775**	773	777	R, C
SG03	1119	1200	1250	**1164**	1150	1169	S
SG04	1219	1250	1300	**1261**	1254	1264	S
SG05	1184	1250	1300	**1084**	1079	1090	S
SG06	1222	1322	1322	**911**	906	915	R, S
SG07	1194	1294	1294	**950**	947	952	S
SG08	1230	1330	1330	**1114**	1109	1119	R, S
SG09	1089	1200	1200	**1173**	1169	1178	S
SG10	1184	1275	1275	**1098**	1091	1105	R, S
SG11	1164	1264	1264	**895**	890	900	R, S
SG12	1284	1384	1384	**1030**	1025	1034	R, S
SG13	1219	1319	1400	**1063**	1060	1065	R, S
SG14	1047	1160	1160	**951**	946	957	S
SG15	1195	1285	1285	**935**	930	940	R, C
SG16	1147	1250	1250	**995**	990	1003	R, S
SG17	1064	1160	1160	**1075**	1072	1079	S
SG18	1042	1142	1142	**859**	856	864	S
SG19	1043	1140	1140	**929**	924	933	S
SG20	1136	1240	1240	**799**	793	805	R, S, C
SG21	1193	1284	1284	**987**	980	990	R, S
SG22	1139	1246	1246	**1145**	1140	1150	S
SG23	1224	1304	1304	**1069**	1064	1074	R, S
SG24	1246	1345	1345	**995**	992	999	R, C
SG25	1233	1333	1333	**1310**	1303	1310	S

(a) The following glasses have identical compositions: SG52 and SG18; SG53 and SG05.
(b) The T_L value was estimated according to the number and size of the crystals observed at T_C.
(c) Primary phases (PP) were S spinel and C clinopyroxene; R indicates the presence of RuO_2 needles.
(d) Glass SG02 was melted three times: twice at 1150°C for 1 h, and then at 1250°C for 2 h.
(e) T_5 is the calculated temperature at which the glass viscosity was 5 Pa·s.
(f) T_{M1} and T_{M2} are the actual melting temperatures of the first and second (third for SG02) melting.
(g) T_C is the highest heat-treatment temperature at which a crystalline phase was found.
(h) T_A is the lowest temperature at which the sample was amorphous after heat-treatment.
Samples were heat-treated in the following furnaces: #1 (SG01,03,05,08-10,17,22-24), #4 (SG11,14-16,19,21), #5 (SG20), #8 (SG04,13,18,25), #9 (SG02,06,07,12).

Table 4.1. Melting and Liquidus Temperatures (in °C) of Test Glasses (cont.)

Glass[a]	T_5[d]	T_{M1}[e]	T_{M2}[e]	T_L[b]	T_C[f]	T_A[g]	PP[c]
SG26	1210	1304	1304	**1071**	1064	1074	S
SG27	1114	1211	1218	**1086**	1079	1090	S
SG28	1037	1150	1150	**833**	829	837	R, C
SG29	1177	1280	1280	**811**	805	816	S
SG30	1045	1157	1157	**1030**	1025	1035	S
SG31	1049	1149	1149	**1081**	1078	1083	S
SG32	1051	1250	1250	**1132**	1129	1135	S
SG33	1045	1145	1145	**943**	939	947	S
SG34	1178	1285	1320	**1282**	1278	1286	S
SG35	1034	1134	1200	**1231**	1225	1235	S
SG36	1168	1265	1265	**813**	809	817	R, C
SG37	1168	1268	1268	**944**	941	950	R, S
SG38	1046	1151	1151	**897**	890	900	S
SG39	1222	1322	1322	**1164**	1160	1168	S
SG40	1205	1300	1300	**1173**	1169	1177	S
SG41	1189	1300	1300	**1304**	1296	1309	S
SG42	1068	1160	1160	**990**	984	997	S
SG43	1219	1317	1317	**924**	922	928	S
SG44	1228	1330	1330	**1244**	1238	1249	R, S
SG45	1217	1317	1317	**936**	932	941	R, S, C
SG46	1094	1257	1250	**1247**	1244	1248	S
SG47	1010	1193	1193	**1144**	1139	1150	S
SG48	1256	1356	1356	**862**	858	869	C
SG49	1221	1315	1315	**877**	872	885	C
SG50	1214	1320	1320	**1285**	1280	1289	S
SG51	1226	1326	1326	**1033**	1031	1035	R, S
SG52	1042	1142	1142	**869**	863	873	R, S
SG53	1184	1284	1284	**1082**	1079	1090	S

(a) The following glasses have identical compositions: SG52 and SG18; SG53 and SG05.
(b) The T_L value was estimated according to the number and size of the crystals observed at T_C.
(c) Primary phases (PP) were S spinel and C clinopyroxene; R indicates the presence of RuO_2 needles.
(d) T_5 is the calculated temperature at which the glass viscosity was 5 Pa·s.
(e) T_{M1} and T_{M2} are the actual melting temperatures of the first and second (third for SG02) melting.
(f) T_C is the highest heat-treatment temperature at which a crystalline phase was found.
(g) T_A is the lowest temperature at which the sample was amorphous after heat-treatment.
Samples were heat-treated in the following furnaces: #1 (SG26,27,30,34,40,41,44,46,47,50,53), #4 (SG38,42,43,49), #5 (SG29,36), #8 (SG28,35,51,52), #9 (31-33,37,39,45,48).

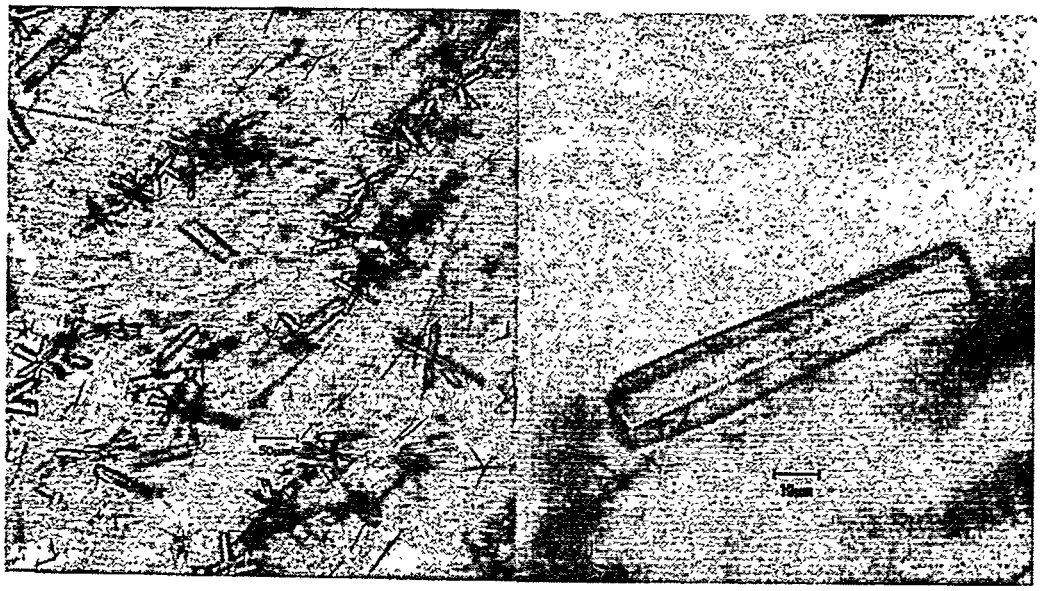

(a) (b)

Figure 4.1. Clinopyroxene Crystals in SG02 Glass at 753°C with RuO_2 Needles (a); a Single Crystal at a Higher Magnification (b)

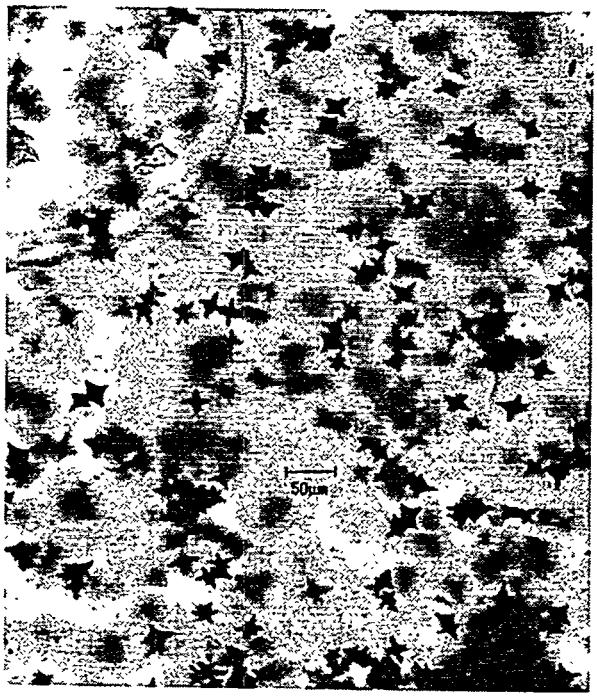

Figure 4.2. Optical Micrograph of Star Shaped Spinel Crystals in SG35 Glass, 1200°C

4.2 Chemical Analysis of Crystals

Some unreported data on spinel composition that were generated in the earlier PNNL SP study [15] are included in this section. These data are of interest because the SP composition region includes or overlaps the ranges of most components relative to the SG composition region. Spinel composition was estimated using SEM energy dispersive spectroscopy (EDS). The results are shown in Table 4.2 for SP-NC-1 glass of the composition (in mass fractions): SiO_2 (0.4677), B_2O_3 (0.0695), Na_2O (0.1381), Li_2O (0.0302), MgO (0.0061), Fe_2O_3 (0.1271), Al_2O_3 (0.0813), Cr_2O_3 (0.0045), MnO (0.0037), NiO (0.0105), and others (0.0623).

The data show that the content of Cr in spinel decreases and the content of Ni and Fe increase as the temperature decreases (as the T_L - T difference increases). The Mn content is low (about 1% in cation fractions) and remains unchanged. Other spinel components, Al and Mg, were detected at 1 to 2% in cation fractions, but not in all samples. Si and Na were also detected in low fractions in only some samples, which could be due to inclusions in spinel crystals or an artifact (smearing).

Table 4.2. Composition of Spinel Crystals (in Cation Fractions, Analyzed by SEM-EDS[(a)]) in SP-NC-1 Glass at Different Temperatures

T, °C	983	1050	1102	1144	1200	1225
Fe	.5146	.5143	.4658	.4646	.4602	.4263
Ni	.2655	.2863	.2603	.2556	.2454	.2333
Cr	.1288	.1686	.1922	.2339	.2668	.2773
Mn	.0123	.0104	.0113	.0143	.0100	.0122
Al	.0189	.0204	-	-	.0176	.0168
Mg	-	-	.0186	.0194	-	-
Si	.0517	-	.0518	.0121	-	.0128
Na	.0082	-	-	-	-	.0213

(a) Averages from 3 to 5 measurements

Chemical analysis was conducted also for spinel isolated from a HLW glass (SS-A glass[20] from a previous study [22]) that precipitated a large quantity of spinel. The glass with spinel was heat-treated, and the spinel was allowed to settle. The sludge was mechanically separated from the spinel-free melt and attacked by nitric acid at 60°C. Spinel crystals were removed from the resulting mixture with silica gel by a magnet. The crystals are shown in Figure 4.3. The chemical analysis of spinel crystals was performed using energy dispersive x-ray fluorescence (EDXRF). Spinel composition is shown in Table 4.3 together with SEM-EDS estimates.

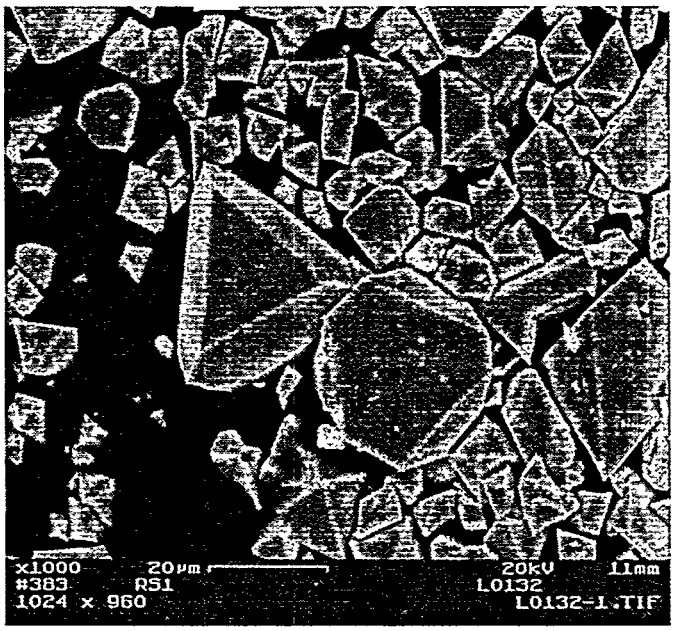

Figure 4.3. Spinel Crystals from a HLW Glass (SEM)

By SEM-EDS analysis, spinel crystals have a higher content of Cr inside than on the surface. This is consistent with the low solubility of Cr_2O_3 in glass, resulting in a tendency of Cr_2O_3 to reach oversaturation before NiO and Fe_2O_3. Because of the low overall Cr_2O_3 content, Cr_2O_3 becomes unavailable when spinel crystals grow over a certain size. Thus, Fe and Ni are at higher concentrations at the crystal surface than towards the center. Both SEM and XRF detected the presence of Al (1 to 2%).[21] The presence of Mg (2 to 3%) was detected only by SEM (its

---

[20] SS-A composition in mass% oxides: SiO_2 42.38, B_2O_3 6.45, Na_2O 14.49, Li_2O 2.77, MgO 1.99, Al_2O_3 7.37, Fe_2O_3 14.08, Cr_2O_3 1.42, MnO 0.33, NiO 3.03 plus other minor components.

[21] Percent of total cations.

atomic mass is too low for detection by EDXRF). EDXRF detected Ru (0.2%) and Rh (0.1%) and also some Cd (<0.1%). SEM did not detect these elements.[22] All analyses detected the presence of Si: SEM about 1% and XRF almost 4%.

Table 4.3. Composition of Spinel Crystals (in Cation Fractions, Analyzed by EDXRF and SEM-EDS) from SS-A Glass

	XRF[a]	1S[b]	2S	3S	4S	AS	1B	2B	3B	4B	5B	6B	AB
Fe	.4223	.4801	.4747	.4986	.4721	.4814	.3998	.4187	.4104	.4363	.4226	.3731	.4102
Ni	.2266	.2801	.2753	.2772	.2590	.2729	.2435	.2492	.2511	.2563	.2514	.2430	.2491
Cr	.2888	.1838	.2041	.1796	.2050	.1931	.2870	.2710	.2688	.2399	.2659	.3063	.2732
Mn	.0083	.0071	.0052	.0067	.0058	.0062	.0069	.0035	.0054	.0106	.0034	.0035	.0056
Al	.0123	.0143	.0132	.0129	.0137	.0135	.0184	.0185	.0220	.0186	.0193	.0237	.0201
Si	.0381	.0084	.0051	.0074	.0176	.0096	.0058	.0058	.0059	.0145	.0056	.0106	.0080
Mg	-	.0262	.0224	.0176	.0268	.0233	.0386	.0333	.0364	.0238	.0318	.0398	.0340

(a) XRF stands for chemical analysis by energy dispersive x-ray fluorescence (EDXRF); this analysis also detected the following cations Ru 0.0019, Rh 0.0011, and Cd 0.0007.

(b) The column headings stand for

1S to 4S	SEM EDS analyses of spinel crystal surfaces
AS	average composition (1S to 4S)
1B to 6B	SEM EDS analyses of spinel in polished thin sections
AB	average composition (1B to 6B)

Capobianco and Drake [24] demonstrated the presence of RuO_2 in spinel . Thus RuO_2 in HLW glasses can exist in four different forms: 1) as undissolved remnants of RuO_2 that formed by the decomposition of ruthenium nitrosylnitrate, $Ru(NO)(NO_3)_3$, used as the batch source of Ru, 2) as a glass component, i.e., RuO_2 dissolved in glass, 3) as needle-like crystals that precipitated from the dissolved RuO_2, and 4) as a component of spinel. Another possible form of

[22] The SEM-EDS detection limit for most elements is 0.05 to 0.1%. It is therefore surprising that SEM did not detect Ru in spinel. The RuO_2 mass fraction in SS-A glass was 0.0003. The glass was melted at 1250°C. No undissolved RuO_2 was found in the rapidly quenched glass. Nevertheless, a possibility exists that some of the Ru detected by chemical analysis of spinel could be RuO_2 that precipitated outside spinel. This RuO_2 could be easily overlooked in the spinel sludge that was used for spinel separation. If this is so, the Ru content in spinel could be below the SEM detection limit. A Ru mass balance study is needed to determine the fraction of Ru in spinel and possible effects of Ru on T_L.

RuO_2 in the waste glass is inclusions of RuO_2 particles within spinel crystals. Such inclusions would result from spinel nucleation on undissolved RuO_2 particles. However, RuO_2 inclusions were not found is spinel, although many attempts were made to detect them by SEM. We can conclude that spinel nucleation on undissolved RuO_2 particles is unlikely to occur (though it is common on RuO_2 needles). The partitioning of RuO_2 between its different forms in waste glass depends on the initial concentration of RuO_2 in the batch, glass composition, temperature, and the fraction of spinel. We understand little of the actual process of RuO_2 partitioning, and no attempt was made to investigate it.

An interesting phenomenon is the presence of a halo around spinel crystals in some brown glasses after a short heat-treatment. This halo was observed in this and previous studies. An example is shown in Figure 4.4. Within the halo, the glass appears colorless. The glass composition within and outside the halo is identical within the accuracy of quantitative EDS (Figure 4.5). The halo is probably caused by a difference in glass redox.[23] FeO likely causes the brown color, whereas only Fe_2O_3 is present within the halo. No attempt was made to further investigate the halo phenomenon.

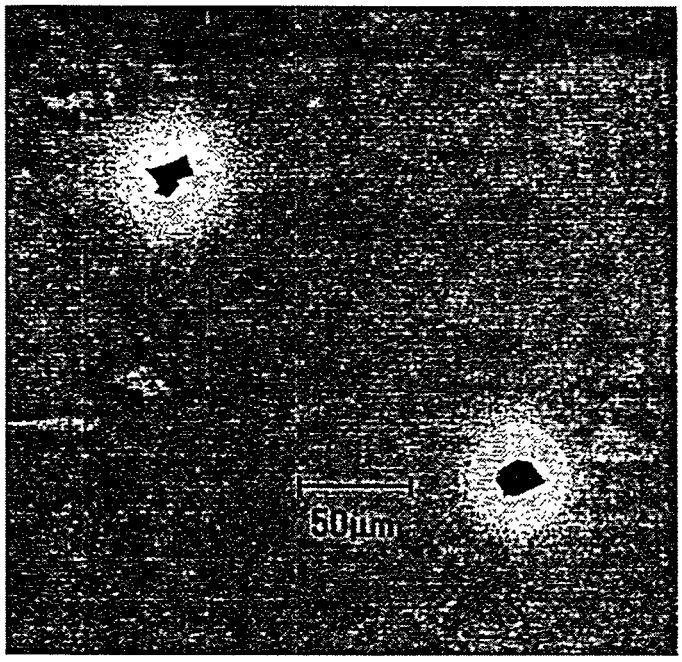

Figure 4.4. Halo Around Spinel Crystals in SG35 Glass

Table 4.4. SG02 Glass Clinopyroxene Composition (in Cation Fractions)[(a)]

Element	#1	#2	#3	#4
Na	0.0891	0.0908	0.0847	0.0936
Mg	0.0833	0.0853	0.0860	0.0948
Ca	0.1055	0.1074	0.1170	0.1145
Ni	0.0033	0.0027	0.0048	0.0065
Mn	0.0134	0.0121	0.0136	0.0131
Fe	0.1484	0.1399	0.1355	0.1229
Cr	0.0062	0.0063	0.0089	0.0051
Si	0.5508	0.5556	0.5495	0.5495

(a) SG02 glass was heat-treated at 753°C for 22 h.

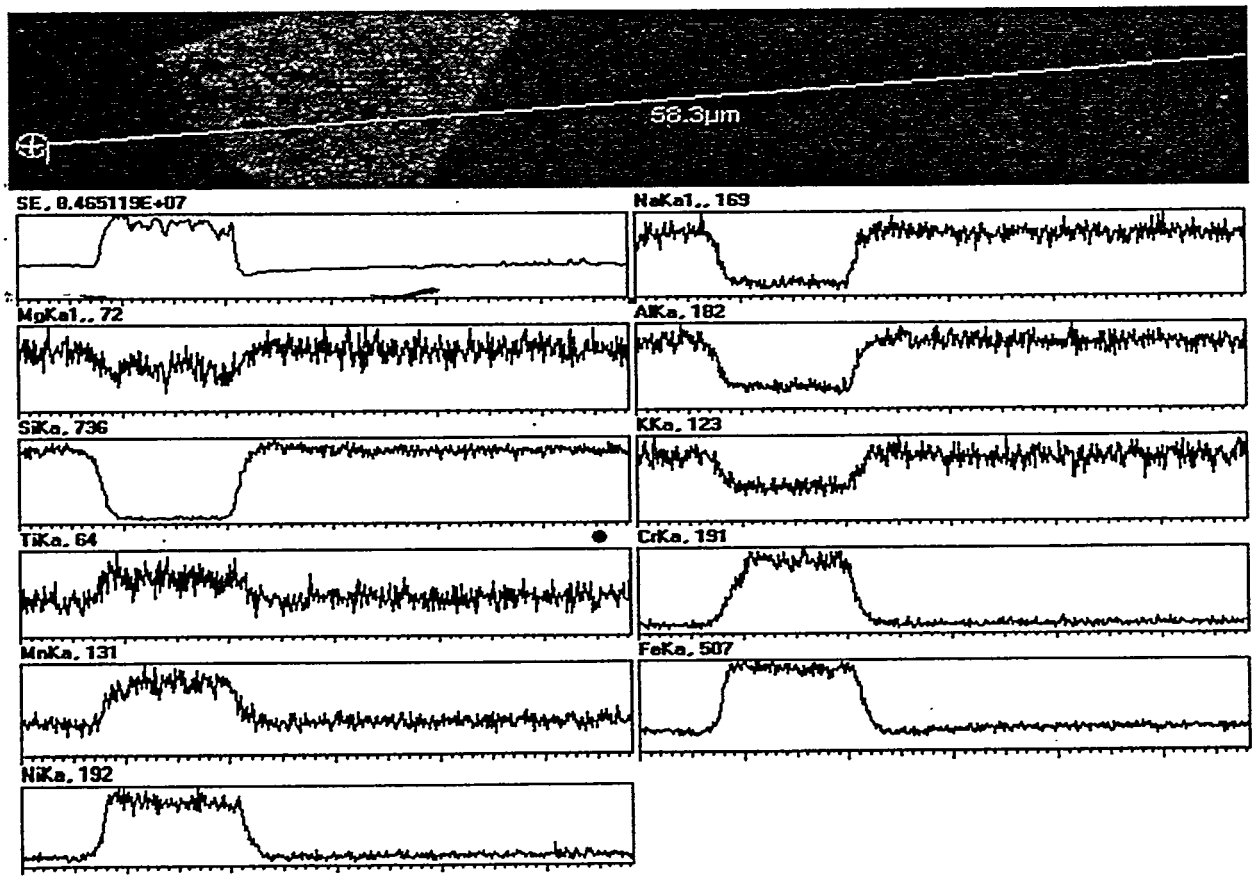

Figure 4.5. SEM-EDS Line Spectra across a Spinel Crystal

[23] D. S. Goldman, "Investigation of Potential Analytical Methods for Redox Control of the Vitrification Process,"

Clinopyroxene formed in many glasses produced in the Hanford Composition Variation Study (CVS) [14,29] and was also identified in this study by optical microscopy and SEM. It occurred in 9 SG glasses as the acmite-augite type of the composition shown in Table 4.4. It did not appear in glasses with <50 mass% SiO_2.

PNL-5581, Pacific Northwest Laboratory, Richland, Washington 1985.

5.0 Data Accuracy, Precision, and Validation

It is crucial that the T_L database is accurate, precise, and reproducible. Three methods were used to assess the accuracy, precision, and validity of the T_L data in this report.

1. An NBS standard glass and a PNNL internal standard glass were tested to assess and adjust for T_L measurement errors (see also Sections 3.3.7 and 5.1).
2. Duplicate glasses were tested to estimate the data uncertainty due to the entire process of glass fabrication and T_L measurement (Sections 3.1 and 5.2). Also, replicate measurements were made on the duplicate glasses to assess the uncertainty of measurements while preparing samples (Section 5.2).
3. T_L results from this study were compared with those from earlier studies to identify any outlying data points and to ensure consistency of the results with past results (Section 5.3).

5.1 Standard Glasses

An NBS standard glass (NBS773) and a PNNL internal standard glass (SP-1)[24] were tested in each furnace used for the T_L measurements. The NBS773 glass certificate, attached as Appendix A, lists a T_L of 991 ± 5°C for the perforated plate method and 988 ± 3°C for the boat method. This specification asserts that 95% of the measured T_L values would fall within the listed ranges for 95% of the glass sample tested. The nominal value for the SP-1 glass is 1040°C.

The T_L values measured in each of the five furnaces (after the completion of the SG study) ranged from 995 to 1018°C for NBS773 and from 1041 to 1073°C for SP-1. These values are clearly larger than the certified NBS773 value and the nominal SP-1 value, indicating some type of bias in the T_L measurement process that appears to depend on the furnaces used. The steps used to adjust for the bias and assess the adjusted T_L values were discussed in Section 3.3.7. The SP-1 glass was chosen as the basis for the adjustment process, and hence its adjusted T_L values are all equal to its nominal value of 1040°C. The adjusted T_L values ranged from 985°C to 997°C for the NBS773 glass. The NBS773 glass was not chosen as the basis for the adjustments because it is not a spinel precipitating glass (SP-1 is). Also, unlike SG and SP glasses, NBS773 glass exhibited surface crystallization. Hence, SP-1 was judged a better choice upon which to base the adjustment process, with the NBS glass used to confirm the success of the adjustment process—see Section 3.3.7.

---

[24] Sections 3.3.6 and 3.3.7.

The adjusted T_L values for NBS773 glass measured in each furnace are 994°C (#1), 991°C (#4), 985°C (#5), 997°C (#8), and 988°C (#9), where the furnace number is supplied in parentheses. Three additional measurements of NBS773 were subsequently made in Furnace #8 at roughly 1-month intervals, yielding 992, 995, and 994°C. Taking the nine measurements as a sample from a single population, we computed a mean of 992°C and a standard deviation of 3.9°C for the pooled data. The mean value, being within the certified range of T_L values for NBS773, indicates that no remaining biases were present after the correction procedure was applied. The standard deviation can be used as an indication of the precision of the measurement procedure.

5.2 Duplicate Glasses and Replicate T_L Measurements

Two sets of duplicate glasses were tested (blind) in this study: SG18 and its duplicate SG52 plus SG05 and its duplicate SG53. Each duplicate glass was batched, melted, and tested as a new test matrix glass according to the procedures in Section 3.2.1. SG18, a vertex composition of the test region with no uranium (see Table 3.2), had a T_L between 856°C and 864°C (estimated 859°C). Its duplicate glass, SG52, had a T_L between 863°C and 873°C (estimated 869°C). SG05, a composition in the center of the test region, had a T_L between 1079°C and 1090°C (estimated 1084°C). Its duplicate glass, SG53, had a T_L between 1079°C and 1090°C (estimated 1082°C). These T_L values are adjusted values, as described in Sections 3.3.7 and 4.1. These differences in duplicate results suggest that the experimental variation in T_L (after furnace adjustments) due to glass batching, sample preparation, and the T_L measurement process is roughly 10°C. This level of variation is in agreement with earlier T_L studies performed at PNNL. For example, SP duplicate glass T_L values differed by 3°C while the measurement uncertainty was 5°C [15].

To test the conjecture that T_L is measured within ± 10°C, T_L measurement was repeated 10 times for SG18 glass and its duplicate SG52. The ASTM sample preparation[25] was performed for five of the measurements, and the PNNL sample preparation was performed for the other five measurements. The ten new T_L results are listed in Table 5.1, along with the previous T_L results for SG18 and SG52 from Table 4.1. Just as the original measurements were adjusted using standard glasses, so were the repeat measurements adjusted. Standards were tested in each furnace, and the results were used to adjust the 10 repeat measurements.

---

[25] See Footnote 15.

Table 5.1. T_L Data (in °C) for Glasses SG18 and SG52

	Original Measurements	Repeat Measurements			
Method	PNNL	PNNL		ASTM	
Furnace Number	8	5[a]	7	5[a]	7
SG18	859	883, 879	891	883, 887	882
SG52	869	883	882	883	891

(a) Furnace 5 is a furnace used to test non-radioactive samples and is different from Furnace 5 used to test radioactive samples (furnace numbering begins from 1 in each of these two areas).

Drawing conclusions from the data in Table 5.1 is complicated by the multiple sources of variation and the unbalanced nature of the data. Potential sources of variation in the data include the time between the original measurements and the repeat measurements,[26] the sample preparation method, the heat-treatment method, the furnace, the duplicate glass, and replicate measurements. The error caused by the heat-treatment method includes the uncertainty in obtaining redox equilibrium with air at T_L and the uncertainty with respect to the concentration of dissolved RuO_2 in the glass—see Section 3.3.6. Not all these variables and their combinations were investigated. Assuming no interactions between or among any of the sources of variation, a statistical analysis of variance found only a statistically significant "time/furnace" effect. The effects of "time" and "furnace" are confounded (i.e., cannot be separated) because only Furnace 8 was used for the original measurements, and only reconfigured furnaces 5 and 7 were used for the repeat measurements.

The largest difference between original and repeat measurements is 32°C (859 to 891°C), while the difference in the means of original and repeat measurements is 20°C (864 versus 884.4°C). This suggests that measurement uncertainties may be as high as ±16°C, considering all sources of error. A majority of this error is thought to be caused by furnace changes due to a laboratory move before the multiple measurements were made.

For the repeat measurements, no statistically significant differences in T_L were found between glasses SG18 and SG52, furnaces 5 and 7, or PNNL and ASTM sample preparation methods. Hence, it was appropriate to treat the 10 repeat measurements as a sample from a single population and compute a mean of 884°C and a standard deviation of 4.0°C. This estimate of the

[26] During this time, the glass testing laboratory was moved to a new building, and some furnace configurations were changed to minimize the differences detected during this study.

precision of the T_L measurement process includes variations due to batching and melting glasses, different furnaces, sample-preparation methods, and T_L determination for a given sample. Generally, it should be expected that most all measurements of the SG18/SG52 glass would be within three standard deviations, roughly ±8 to ± 12°C.

5.3 Data Evaluation

The data, and quantities derived from the data, from this study are compared in this section to results from other studies to assess consistency.

5.3.1 Partial Specific Liquidus Temperatures

The partial specific liquidus temperatures, T_{Li}, were obtained from experimental data using the equation

$$T_L = \sum_{i=1}^{N} T_{Li} g_i \qquad (2)$$

where g_i is the i-th component mass fraction from as-batched composition and N is the number of components. This process has the following advantages:

- identifying outlying data points for further analyses
- determining if the T_{Li} values are consistent with those from other data sets
- determining if the data in this report can be combined with data generated for Hanford glasses to form a single, larger, database.

The T_{Li} values were obtained for the SG database from this study and the SP database from a previous HLW glass study [15]. The composition regions of these databases are different—see Table 3.1. The SG database consists of 51 distinct glass compositions (see Table 3.2), 44 of which precipitated spinel as the primary crystallization phase. The 44 glasses do not include SG20 and SG45, which precipitated both spinel and clinopyroxene. The multiple measurements for SG18 and SG52 were added to give a total of 54 data points in the SG data set. The SP database consists of 33 glasses, all of which precipitated spinel as the primary crystallization phase. The SP study varied the glass composition one-component-at-a-time around a baseline glass. The SG study used a layered statistical design [32], including compositions on the boundary, interior, and center of the composition region. However, because 7 of the SG glasses did not precipitate spinel as the primary phase, the composition region coverage of the layered design may be somewhat compromised.

A third database, SG&SP, of 87 glasses was created by combining glasses from these two studies. As seen in Table 3.1, the component ranges in the SP study were wider (sometimes much wider) than the SG component ranges for some components (SiO_2, B_2O_3, MgO, MnO, NiO, Fe_2O_3, Cr_2O_3), partially overlapped for other components (Al_2O_3, Na_2O), and did not overlap at all for one component (Li_2O). Further, the SG study varies several components (K_2O, CaO, TiO_2, U_3O_8) not varied in the SP study. The differences in components and component ranges between the SG and SP studies is sufficient to warrant caution in combining or comparing results from the two studies. Still, there is enough commonality to proceed with such comparisons. T_{Li} values for these three databases are listed in Table 5.2.

Table 5.2. Partial Specific T_L Values (T_{Li}) in °C

	SG	*SP*	*SG&SP*
Al_2O_3	2614	3307	2866
B_2O_3	485	395	403
CaO	2075		1757
Cr_2O_3	24670	18864	20592
Fe_2O_3	2632	2644	2685
K_2O	-1324		-980
Li_2O	-1462	-1470	-1367
MgO	4857	2827	3820
MnO	888	1870	1312
Na_2O	-1624	-1826	-1736
NiO	9661	8210	9530
SiO_2	1021	834	1010
TiO_2	4301		4925
U_3O_8	1546		1633
Others		4419	3583
R^2	0.96	0.94	0.95
s (°C)	32.3	25.0	31.6

Table 5.2 also shows R^2 and s values for the overall fits of Equation (2) to the three databases. R^2 is the fraction of the variation in T_L database values accounted for by the equation. The quantity s is the root mean square error and estimates the experimental error standard deviation if Equation (2) does not have a significant lack of fit. The R^2 values listed in Table 5.2 suggest that Equation (2) provides reasonable approximations to the relationships between glass composition and T_L for each of the three databases. The s values listed in Table 5.2 range from 25.0°C to 32.3°C, being larger than the imprecision standard deviation of 4°C.

Before using Equation (2) with the coefficients in Table 5.2, we must confirm they reasonably approximate the T_L-composition relationships for each of the three databases. This topic is discussed in the following section.

5.3.2 Outliers

To assess the performance of the fitted equations with the partial specific properties in Table 5.2, T_L values were calculated using the equations and plotted versus the measured T_L values. Such plots are also useful for identifying outlying data points. Figure 5.1 displays the calculated versus measured T_L plot for Equation (2) fitted to the SG database.

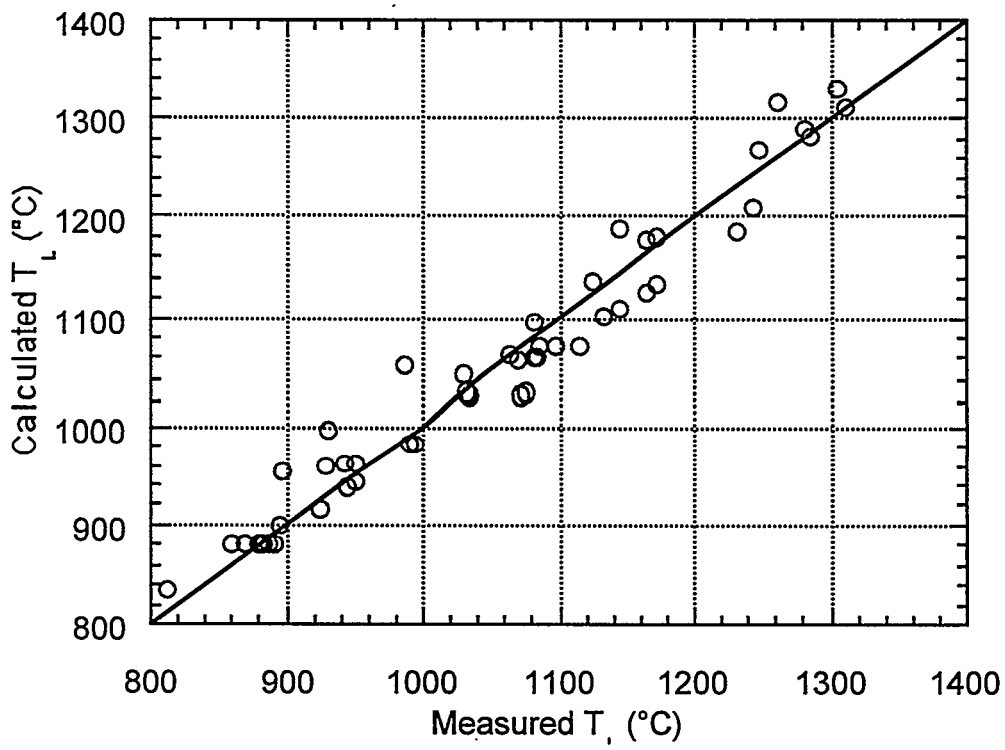

Figure 5.1. Calculated Versus Measured T_L Values for SG Glasses

The SG data appear to be well represented by the calculated T_L values with no obvious outliers. The Cook's D influence[27] for these data varied from 6.7×10^{-7} to 0.397. Only two data points had a Cook's D influence greater than 0.25: SG47 with 0.279 and SG06 with 0.397. The

[27] A statistic used to identify data points with large influence on the least squares fit to a data set.

lowest Cook's D influence values were for duplicate measurements of SG18 and SG52 followed by SG25. Cook's D values can be large because of an outlying or influential response (T_L) value, or because the composition's position is outlying or influential. With a designed experiment, the composition should not be outlying, but it may be influential because of representing a more extreme portion of composition space (possibly because of compositions "lost" due to not having spinel as the primary phase). The T_L of SG06 was re-measured to investigate the reason for its influence. The initial measurement for SG06 (Table 4.1) was between 906 and 915°C (estimated 911°C). The re-measured T_L value for SG06 was between 927 and 937°C (estimated 931°C). Refitting Equation (2) with the adjusted SG06 value decreased the Cook's D influence value to 0.303 and made no noticeable difference in T_{Li} values. The T_L of SG47 was confirmed by analyses of existing samples and was not re-measured (SG47 is a uranium-containing glass that would take significant effort to re-measure).

Based on the estimates of variation in measurement described in Section 5.2, it is not clear if the differences between the two measured values of SG06 T_L (911 and 931°C) are typical or if they stand out as the Cook's D influence would suggest. A question arises: was the first measurement of SG06 in error and the second measurement correct or should both values be considered correct? The T_L value of SG25 was also re-measured to help determine if SG06 could be regardless a typical glass or an outlier. The initial measurement for SG25 (Table 4.1) was between 1303 and 1310°C (estimated 1310°C). The re-measured T_L value for SG25 was between 1304 and 1314°C (estimated 1309°C). The difference between the T_L values for SG25 was small (1°C), whereas the difference in SG06 values was 20°C. The three standard deviation value of ±12°C is a measure of imprecision. A larger difference than that suggests that there was a bias involved in one or both of the measurements of SG06 or that there is something about the SG06 composition that causes higher imprecision in measuring T_L.

5.3.3 Comparison of Data Sets

To assess data consistency and to determine the applicability of SG data for use in Hanford glass development and vice versa, the SG and SP data sets were compared. Figure 5.2 compares the T_L values calculated using Equation (2) and the SG T_{Li} values to the measured T_L values for the SG and SP data sets. The SP data falls under the 45° line by roughly 150°C.

Figure 5.3 compares the T_L values calculated using Equation (2) and T_{Li} values from the SP data set to measured T_L values for the SG and SP data sets. The T_L values for the SG glasses are underpredicted by roughly 150°C. These observations are encouraging since there is apparently a constant variation in T_L between the two data sets. This constant difference may be caused by

varying components in one data set and not the other, or it may be due to the difference in the SG and SP composition regions studied.

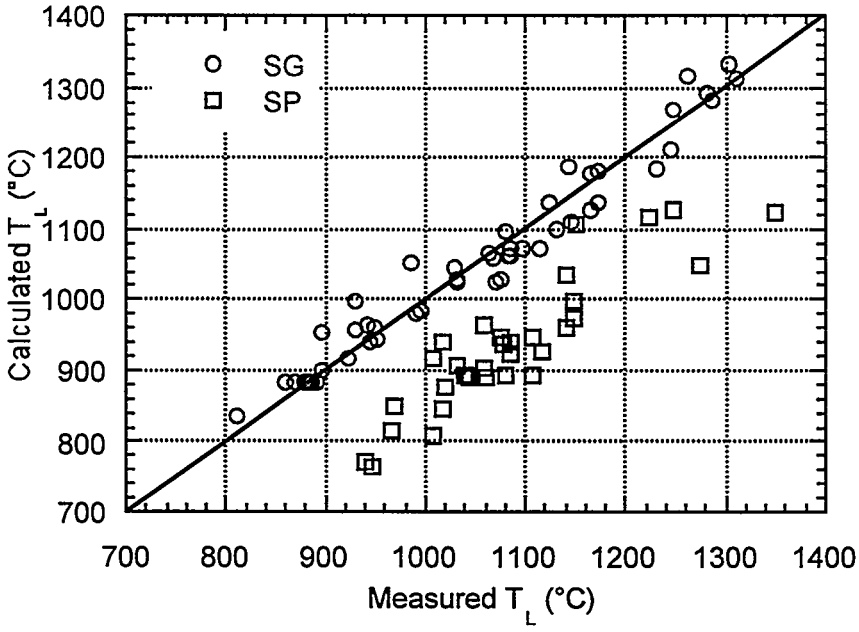

Figure 5.2. Calculated (Using SG T_{Li} Values) Versus Measured T_L Values for SG and SP Glasses

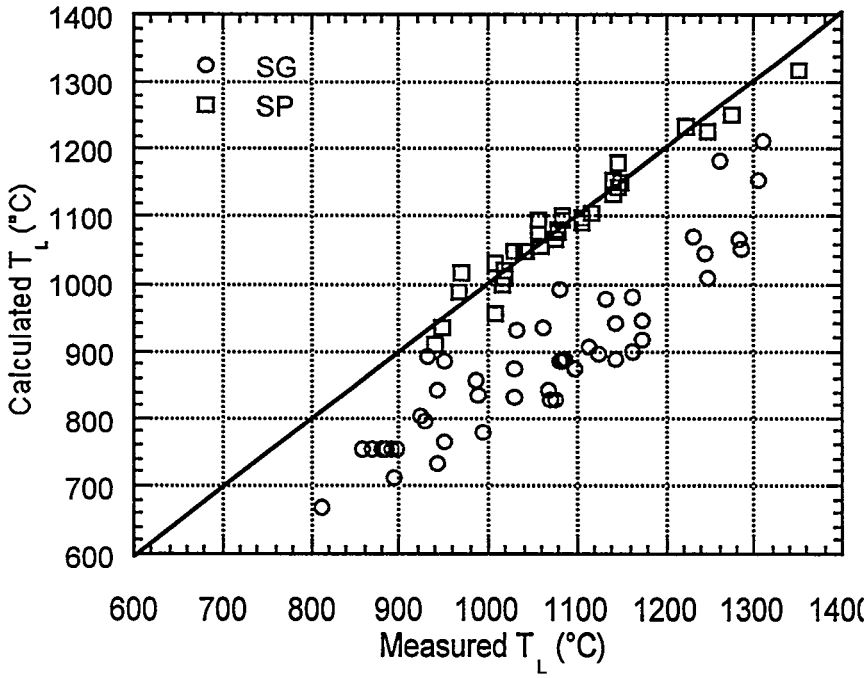

Figure 5.3. Calculated (using SP T_{Li} values) Versus Measured T_L Values for SG and SP Glasses

Figure 5.4 compares the measured T_L values for the SG and SP data sets with the calculated values using SG&SP T_{Li} coefficients. As expected by the linear offset between the two data sets, Equation (2) with T_{Li} values from the SG&SP data set represents the measured values very well.

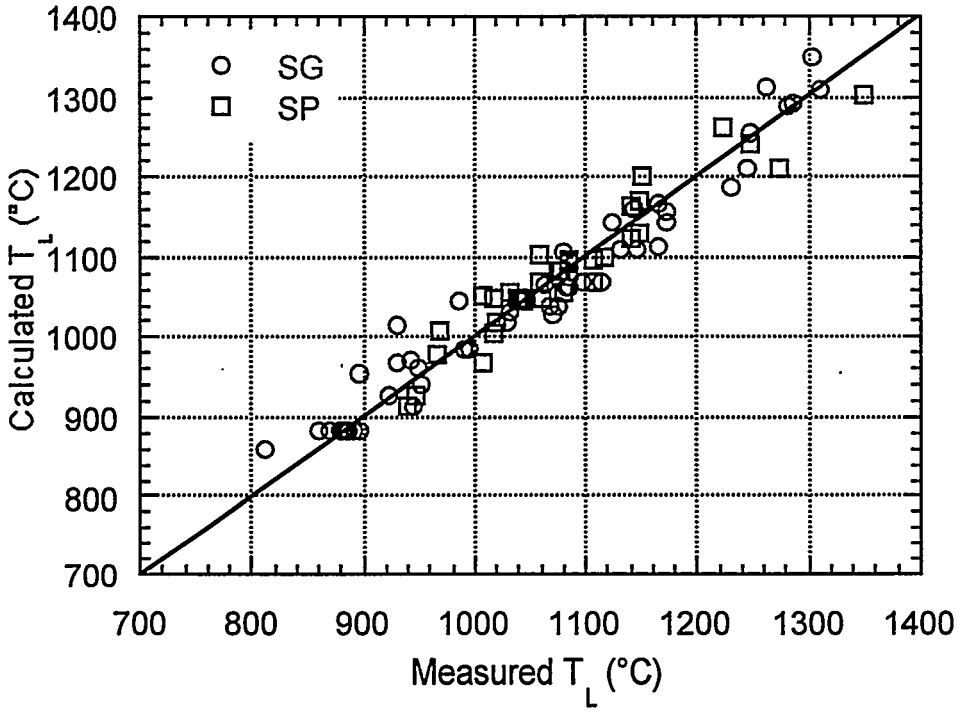

Figure 5.4. Calculated (Using SG&SP T_{Li} Values) Versus Measured T_L Values for SG and SP Glasses

The differences between T_{Li} values for each i-th component in Table 5.2 are partially caused by the differences in the SG and SP composition regions. Alternatively, we can compare estimates of the component effects (slopes) along the directions of adding each component to a reference composition. The component effects and their standard deviations were obtained by fitting the equation

$$T_L = T_{L,ref} + \sum_{i=1}^{N} S_i z_i \qquad (3)$$

such that $\sum_{i=1}^{N} S_i z_i = 0$, to the SG, SP, and SG&SP data sets via constrained least squares regression. In Equation (3), $T_{L,ref}$ is the estimated T_L at the reference composition SG05, S_i is the

slope of the i-th glass component along the direction of adding component i to the reference composition, and $z_i = 100(1 - r_i)g_i$, where g_i is the mass fraction of the i-th glass component and r_i is the mass fraction of the i-th component of the reference composition.

It can be shown that

$$S_i = \frac{T_{Li} - T_{L,ref}}{100(1 - r_i)} \quad (4)$$

The slope S_i represents the estimated change in T_L for a 1 wt% change in component i. For components with less than a 1 wt% range, a proportionally smaller change in T_L is all that can occur.

The results of fitting Equation (3) to the SG, SP, and SG&SP data sets with SG05 as the reference glass are listed in Table 5.3. Only 53 of the 54 SG data points were used because SG06 was omitted as an outlier. A total of 43 SP data points was used, 10 more than the 33 used to produce the SP results in Table 5.2. The additional 10 points consisted of 8 replicates of the SP-1 glass, and 2 glasses in which RuO_2 was varied along the direction of adding it to the SP-1 reference composition. The combined SG&SP database used to produce the results in Table 5.3 consists of 96 data points. This number of points is 9 more than used to produce the results of Table 5.2 due to omitting 1 SG glass and adding 10 SP glasses. The data differences cause the R^2 and s values listed in Table 5.3 to differ slightly compared to the values listed in Table 5.2. The values would be exactly the same if the data were the same because Equations (2) and (3) provide mathematically equivalent fits.

The 1222°C to 1084°C = 138°C overprediction of T_L at SG05 for the SP data set is somewhat unsettling at first. However, the SG05 composition has several components with proportions near (Al_2O_3, CaO, Cr_2O_3, and Na_2O) or beyond (K_2O, Li_2O, U_3O_8, and TiO_2) the extremes of the corresponding component ranges in the SP study. Also, the SP study only varied components along directions of component addition/subtraction to/from the SP-1 composition. Thus, SG05 is extreme in the SP composition region where there are no data and where there is likely significant departure from linear blending based on previous analyses of the SP data. The 138°C overprediction explains the behavior seen in Figure 5.3.

For components varied in both the SG and SP studies, the slopes in Table 5.3 are similar except for MgO (which has a stronger effect for SG than SP) and SiO_2 (which has a stronger effect for SP). MnO appears to have a negligible effect on spinel T_L in both the SG and SP studies, while RuO_2 has a negligible effect for SP, and SiO_2 has a negligible effect for SG. The

slopes in Table 5.3 for the SG&SP data set fall between the values for the separate data sets. Assessments of component effects based on Table 5.3 should only be taken very generally because of indications that Equations (2) and (3) have some lack of fit in approximating the T_L-composition relationships.

Table 5.3. Component Effects (Slopes) Along the Directions of Adding Components to the SG05 Glass Composition

	SG		SP		SG&SP	
Component	S_i	$s(S_i)$	S_i	$s(S_i)$	S_i	$s(S_i)$
$T_{L(SG05)}$	1058.8	5.16	1222.3	30.07	1059.4	4.72
Al_2O_3	18.14	1.90	22.25	2.45	20.28	1.52
B_2O_3	-7.71	2.13	-9.29	2.25	-8.17	1.61
CaO	11.70	6.23			11.16	5.90
Cr_2O_3	261.01	53.04	180.55	20.25	200.18	21.24
Fe_2O_3	18.34	1.20	15.45	3.13	18.67	1.14
K_2O	-19.97	4.48			-18.19	4.32
Li_2O	-28.25	3.44	-29.54	6.78	-27.71	3.08
MgO	33.37	5.30	17.03	4.31	25.71	3.58
MnO	-5.63	5.12	7.55	6.44	-1.03	4.23
Na_2O	-28.68	2.10	-33.60	2.52	-29.66	1.57
NiO	84.72	5.25	71.80	9.24	82.56	4.63
RuO_2			299.99	223.81	144.15	224.48
SiO_2	-1.14	1.12	-7.98	1.67	-1.39	0.92
TiO_2	42.19	23.11	33.98	11.49	43.18	22.55
U_3O_8	3.81	1.89			3.95	1.90
Others			33.98	11.49	21.50	4.10
R^2	0.97		0.94		0.96	
s	26.8		23.47		27.03	

5.4 Summary of Accuracy, Precision and Consistency

Based on the work discussed above, the database presented in this report is of good accuracy and precision and is consistent with the database from the SP study for Hanford glasses. The following observations can be made:

- The mean of multiple measurements of the NBS773 standard glass was found to be 992°C, which is within the range reported in the glass Certificate (Appendix A).
- The standard deviation of multiple measurements of the NBS773 glass was 3.9°C.

- Replicate glasses had T_L values with differences ranging from 1 to 32°C. The standard deviation of multiple measurements of replicate glasses was 4.0°C.
- One outlier (SG06) was found in calculating partial specific T_L values for the SG data set. A 20°C difference in T_L values from the original and subsequent measurement was found.
- A constant difference of roughly 150°C was seen between measured T_L values in the SG data set and calculated T_L values based on the SP data set (and vice versa). This appears to be due to differences in components and component ranges between the two studies.
- A combined SG&SP data set showed consistency, suggesting that the data can be combined for developing T_L-composition relationships for DWPF and Hanford.
- With a few exceptions, the effects on T_L of components varied in both the SG and SP studies are quite similar, suggesting that the SG data set is consistent with the SP data set.

An assessment of the measurement imprecision suggests that most glasses are expected to have T_L values within the range of ± 8°C or ± 12°C of the measured values in Table 4.1, based upon two or three standard deviations from glasses measured multiple times. An assessment of the possible causes for the variation in measured data is discussed in the following section.

6.0 Discussion

This section is concerned with two questions: how do individual glass components affect T_L, and what are possible sources of errors in T_L measurement? Apart from being of general interest, the knowledge of component effects is important for glass formulation work to optimize waste loading while keeping T_L low enough for safe processing. These effects are discussed for individual glass components in Section 6.1. The possible sources of errors stem from general imperfections, such as batch dusting, temperature fluctuations, or glass volatility. More importantly, errors may result from influential variables that were not part of experimental design (RuO_2 concentration and redox). Possible sources of errors are discussed in Section 6.2.

6.1 Component Effects

Using the expression $\sum_{i=1}^{N} g_i = 1$, from which $g_n = 1 - \sum_{i=1}^{N-1} g_i$, Equation (2) can be transformed to:

$$T_L = T_{L,n} + \sum_{i=1}^{N-1} (T_{Li} - T_{Ln}) g_i \qquad (5)$$

The difference $T'_{Li} = T_{Li} - T_{Ln}$ is called the i-th component relative partial specific liquidus temperature. The numerical value of $T'_{Li}/100$ expresses a change in T_L that results from replacing 1 mass% of the n-th component (such as SiO_2) by 1 mass% of the i-th component. This is one of the possible measures of the i-th component's effect (another is the effect of adding of 1 mass% of the i-th component to the mixture discussed in Section 5.3.3).[28] SiO_2 is a good choice for the n-th component because it is the most abundant component in the glass. The following sections discuss the effects on T_L of individual glass components replacing SiO_2. We need to stress that the numerical values of these effects (such as relative partial specific liquidus temperatures) are mere estimates from fitting to data the linear Equation (2) that is likely

[28] Assessing component effects relative to a 1 mass% change is done as a matter of standardization and convenience. For a component with range smaller than 1 mass%, such a standard measure of the component effect will be too large. This can be recognized in assessing such standard measures of component effects.

inadequate because of nonlinear blending. The T_{Li} values used for the following discussion are listed in Table 5.2.

6.1.1 Effect of Cr_2O_3

As Table 5.2 shows, Cr_2O_3 has an extremely strong effect on T_L [26]. This effect is stronger for SG glasses than for SP glasses. Replacing 1 mass% SiO_2 with 1 mass% Cr_2O_3 results in a T_L increase by roughly 200°C. The $T_{L,Cr}$ value for the SG region is subject to a high degree of uncertainty because Cr_2O_3 varied within a narrow range of 0.1 to 0.3 mass% (Table 3.1). A somewhat wider Cr_2O_3 range, from 0 to 1.2 mass%, was tested in the SP study.

A closely related subject is the solubility of Cr_2O_3 in glass as a function of composition and temperature. Approximately 1 mass% Cr_2O_3 can be dissolved in HLW glasses at temperatures around 1150°C. The actual Cr_2O_3 solubility varies according to glass composition. Cr_2O_3 solubility increases with the increasing concentration of alkali oxides in glass and decreases with the increasing concentration of NiO, MgO, Al_2O_3, and Fe_2O_3 in glass. The form at which Cr_2O_3 precipitates also depends on glass composition and varies from escolaite to corundum to spinel; Cr_2O_3 can also be a component of clinopyroxene. Because approximately 1 mass% Cr_2O_3 can be dissolved in a HLW glass at temperatures around 1150°C, the melting temperature of DWPF glass (with 0.1 to 0.3 mass% Cr_2O_3) is not restricted by the presence of Cr_2O_3. No undissolved Cr_2O_3 was ever observed in any DWPF glass; all the batched Cr_2O_3 was either dissolved or reacted with other glass components to form spinel or clinopyroxene.

A word of caution is appropriate when preparing glasses with a high Cr_2O_3 content in the laboratory. In atmospheric air, Cr_2O_3 oxidizes to chromate at temperatures above 200°C [33]. Above 600 to 700°C, chromate is reduced back to Cr_2O_3. Chromate is a yellowish green liquid that tends to segregate on the top of the melt and spread over crucible walls. This behavior may be a source of uncertainty in determining the effect of Cr_2O_3 on T_L.

6.1.2 Effect of NiO

Nickel oxide also strongly increases T_L, though not as much as Cr_2O_3. NiO varied from 0.05 to 2 mass% in SG glasses (to 3 mass% in SP). Both SG and SP data yield similar values of $T_{L,Ni}$. Replacing 1 mass% SiO_2 with 1 mass% NiO increases T_L roughly by 80°C.

6.1.3 Effect of Fe_2O_3

The third oxide that forms spinel, Fe_2O_3, also increases T_L, but much less than Cr_2O_3 and NiO, and less than MgO and TiO_2. The span of Fe_2O_3 concentration was the same for SG and SP studies, 6 to 15 mass%. Replacing 1 mass% SiO_2 with 1 mass% Fe_2O_3 increases T_L by approximately 17°C. This small effect of Fe_2O_3 on T_L within the spinel field indicates that Cr_2O_3 and NiO are the active components that start spinel precipitation on cooling. Although a spinel (magnetite, Fe_3O_4) can precipitate from iron-rich glass in the absence of Cr_2O_3 and NiO, maghemite (Fe_2O_3) is more likely to form [27]. The dependence of spinel composition on the temperature at which spinel precipitates from glass (Section 4.2) indicates that at temperatures just below T_L, Cr_2O_3 reacts with NiO and Fe_2O_3, forming a solid solution of nichromite ($NiCr_2O_4$) and chromite ($FeCr_2O_4$). This solid solution is increasingly enriched by trevorite ($NiFe_2O_4$) and magnetite as temperature decreases.

6.1.4 Effect of MgO and CaO

The relatively strong effect of MgO on T_L within the spinel primary field of HLW glasses is well known [16]. MgO varied from 0.5 to 2.5 mass% in SG glasses (to 6 mass% in SP). Replacing 1 mass% SiO_2 with 1 mass% MgO increased T_L by 20 to 40°C. CaO affects T_L less than MgO. Replacing 1 mass% SiO_2 with 1 mass% CaO will increase T_L by approximately 10°C.

6.1.5 Effect of Al_2O_3

Another oxide that increases T_L within the spinel field is Al_2O_3. Al_2O_3 varied from 2.5 to 8 mass% in SG glasses (from 4 to 15 mass% in SP). Replacing 1 mass% SiO_2 with 1 mass% Al_2O_3 increased T_L by 16 to 25°C. MgO and Al_2O_3 form spinel at high temperatures and are minor components in spinel that precipitates from HLW glass below 1300°C (Section 4.2).[29]

6.1.6 Effect of TiO_2

TiO_2 was not varied as a component in the SP series. Replacing 1 mass% SiO_2 with 1 mass% TiO_2 in SG glasses increased T_L by approximately 30 to 40°C. Considering the extremely narrow range of TiO_2 concentration, 0.15 to 0.6 mass% in SG glasses, this effect is less certain than that of other glass components.

---

[29] Spinel containing MgO and Al_2O_3 formed at 1050-1100°C in glasses for plutonium immobilization. See J. D. Vienna, R. P. Thimpke, G. F. Piepel, M. L. Elliott, R. K. Nakaoka, and G. W. Veazey, "Glass Development for Treatment of Evaporator Bottoms Waste," PNNL report, to be issued in 1998.

6.1.7 Effect of MnO

Another spinel-forming component, MnO, increases T_L only slightly. A 1 mass% addition of MnO at the expense of SiO_2 increased[30] T_L by 0 to10°C. MnO varied in the SG matrix from 1 to 3 mass% (to 4 mass% in SP).

6.1.8 Effect of U_3O_8

Uranium oxide, U_3O_8, exhibited little effect on T_L (see also Section 5.3.3). Its concentration in SG glasses was 0 to 5.5 mass% (SP glasses did not contain uranium). Replacing 1 mass% SiO_2 with 1 mass% U_3O_8 increases[31] T_L by approximately 6°C.

6.1.9 Effect of RuO_2

Schreiber [28] found less than 0.001 mass% RuO_2 dissolved in a HLW borosilicate glass melted at 1200°C. The RuO_2 solubility limit is probably higher at temperatures above 1200°C in glasses tested in this study. Melting these glasses at elevated temperatures substantially reduced the concentration of undissolved RuO_2 as described in Section 3.3.1. This decrease in undissolved RuO_2 can be attributed partly to the agglomeration of RuO_2 particles and their subsequent settling and partly to dissolution.[32] The existence of RuO_2 needle-like crystals that precipitated from some glasses indicates that some RuO_2 has dissolved.

RuO_2 is a spinel component (see Section 4.2) that is even less soluble in glass than Cr_2O_3. As the glass cooled, the dissolved RuO_2 could either precipitate as needle-like crystals or become a component in spinel as a direct chemical analysis of spinel crystals separated from glass (Table 4.3) suggests. Though its concentration (probably < 0.01% on a cation basis) was too low to be detectable by SEM-EDS, it might be high enough to influence spinel formation in glass and thus to affect T_L within the spinel field.

The effect of RuO_2 on T_L could not be established with SG and SP glasses because its concentration was not varied in these studies. SG glasses contained a constant concentration of

---

[30] Considering the uncertainty of measured T_L values, the uncertainty of test matrices in representing their respective composition regions, and the nonlinear behavior of mixtures, it is not certain whether small-to-negligible effects actually do increase or decrease T_L of concrete glass compositions within the region.

[31] See previous footnote.

[32] The evaporation of RuO_2 during remelting was considered negligible. However, no attempt was made to prove that experimentally.

0.09 mass% RuO_2 and SP glasses of 0.03 mass% RuO_2. Nevertheless, RuO_2 is partly soluble in HLW glasses and may affect T_L. As the component effects listed in Table 5.3 suggest, the effect of RuO_2 on T_L is comparable to that of Cr_2O_3.

6.1.10 Effects of SiO_2 and B_2O_3

T_L values for spinel in SG glasses range from 865°C to 1316°C, and the SiO_2 coefficient is 981°C. Therefore, silica has virtually no effect on T_L within the spinel primary field. B_2O_3 decreases T_L slightly, by approximately 5°C if 1% B_2O_3 is added at the expense of SiO_2.

6.1.11 Effects of Alkali Oxides

Alkali oxides decrease T_L. Na_2O has the strongest effect, similar to Li_2O and somewhat stronger than K_2O. A 1 mass% addition of Na_2O at the expense of SiO_2 decreases T_L by approximately 27°C, a 1 mass% addition of Li_2O decreases T_L approximately by 24°C, and a 1 mass% addition of K_2O decreases T_L approximately by 20°C. Alkali oxides varied in SG glasses as follows: Na_2O 6 to 11 mass% (8 to 20 mass% in SP), Li_2O 3 to 6 mass% (0 to 3 mass% in SP), and K_2O 1.5 to 3.8 mass% (absent in SP).

The effects of Na_2O and Li_2O on T_L were similar in both studies (SG and SP), even though K_2O was absent in SP glasses. Therefore, there is no evidence of interaction between K_2O and the other two alkali oxides (a mixed alkali effect). Also, a similar effect of Li_2O on T_L in SG and SP glasses despite its different concentration ranges indicates the absence of any strong nonlinearity in the effect of Li_2O. These observations are provisional and need more data.

6.1.12 Effects of Other Components

While SG glasses had only 14 components, SP glasses had a large number of minor components and one major component, ZrO_2, whose effect on T_L was not investigated separately from minor components. The effect of ZrO_2 and minor components taken together as Others is significant. Replacing 1 mass% SiO_2 by ZrO_2 plus minor components increases T_L by 26 to 36°C. Explaining this large effect will be important for Hanford HLW glass.

6.1.13 Effect of Glass Composition on T_{Li}

Partial specific properties are generally functions of composition. The values in Table 5.2 are approximations of T_{Li} values as constants. Geometrically, the liquidus surface of the portion of the spinel field covered by SG and SP data was approximated as a hyperplane. Second-order effects were estimated via regression analysis of the SG&SP data. Several significant squared

terms (a positive squared term for Al_2O_3 and negative squared terms for NiO, MgO, and K_2O) were identified. A significant positive cross-product term was obtained for $Cr_2O_3 \times NiO$. However, it is beyond the scope of this work to further pursue the investigation of nonlinear blending effects of components.

6.1.14 Component Effects Summary

The goal of glass formulation is to increase waste loading without imposing unacceptable risks on melter operation. In terms of liquidus temperature, T_L should be as close as possible to 1050°C, which is the conventional limit for Joule-heated melters. In a glass with T_L = 1050°C, an addition of a component with T_{Li} > 1050°C will increase T_L, whereas an addition of a component with T_{Li} < 1050°C will decrease T_L. Accordingly, glass components for both the SG and SP databases can be arranged into four groups:

$$(Cr_2O_3, NiO) >> (MgO, TiO_2, Al_2O_3, Fe_2O_3) > (U_3O_8, MnO, CaO, B_2O_3, SiO_2) > (K_2O, Li_2O, Na_2O)$$

Components in the first group (Cr_2O_3 and NiO) strongly increase T_L. Components in the second group (MgO, TiO_2, Al_2O_3, and Fe_2O_3) moderately increase T_L. Components in the third group (U_3O_8, MnO, CaO, B_2O_3 and SiO_2) have little effect on T_L. Components in the fourth group, consisting of alkali oxides (K_2O. Li_2O, and Na_2O), decrease T_L.

An example of a glass with a high waste loading and T_L below (yet close to) 1050°C is shown in Table 6.1. T51-opt-U glass has an elevated concentration of 41 mass% SRS Tank 51 sludge-only HLW and T51-opt glass is its uranium-free version that was prepared in the laboratory. An optimized four-component frit (SiO_2-B_2O_3-Na_2O-Li_2O) was developed for this waste using property-composition relationships [8,10,25]. Measured and calculated T_L values for T51-opt are shown in Table 6.1. Although T51-opt glass is outside the SG region for Na_2O, Li_2O, and K_2O and outside the combined SG&SP region for Fe_2O_3, the difference between measured and calculated T_L is only 18°C.

Table 6.1. Composition (in Mass Fractions) of Waste, Frit, and T51-opt Glasses

Oxide	Waste	Frit	T51-opt-U	T51-opt
Al_2O_3	0.1509		0.0619	0.0628
B_2O_3	0	0.0847	0.0500	0.0508
CaO	0.0447		0.0183	0.0186
Cr_2O_3	0.0029		0.0012	0.0012
Fe_2O_3	0.4863		0.1994	0.2024
K_2O	0.0015		0.0006	0.0006
Li_2O	0	0.018	0.0106	0.0108
MgO	0.0264		0.0108	0.0110
MnO	0.0459		0.0188	0.0191
Na_2O	0.1567	0.1962	0.1800	0.1827
NiO	0.0043		0.0018	0.0018
SiO_2	0.0185	0.7011	0.4213	0.4276
TiO_2	0.0008		0.0003	0.0003
U_3O_8	0.0361		0.0148	
Others	0.0248		0.0102	0.0103
Measured T_L				1039
Calculated T_L				1021

6.1.15 Effect of Melting Temperature

The high RuO_2 content in SG glasses prevented the optical detection of spinel when the glass was melted at T_5. To allow a reliable detection of spinel, we reduced the occurrence of undissolved RuO_2 in SG glasses by melting them at a temperature ≥ 100°C above T_5. This, however, lead to a necessity to re-equilibrate the glass with the air oxygen during the sample heat-treatment that could take place at a temperature several hundred °C lower than that at which the glass was melted. Naturally, a question arises: if SG glasses had a lower RuO_2 content and were melted at a lower temperature, would this difference have any impact on the measured T_L? To answer this question, we re-batched SG06 and SG25 glasses with 0.03 mass% RuO_2 and melted them at T_5. The samples were heat-treated for T_L measurements together with SG06 and SG25 glasses with 0.09 mass% RuO_2 and melted them at T_5 + 100°C. The results are shown in Table 6.2. As this table shows, the T_L values are within the ± 12°C error. This is surprising because we would expect an impact of the low RuO_2 content on T_L (see Section 6.1.9). We made no attempt to clarify this issue still further by melting glasses with 0.03 mass% RuO_2 at T_5 + 100°C.

Table 6.2. Effect of Melting Temperature on T_L (Temperatures in °C)

		SG06	SG25
	T_5	1222	1233
Original Measurement,	T_{M2}	1322	1333
0.09 mass% RuO_2	T_L	911[(a)]	1310
Repeated Measurement,	T_{M2}	1322	1333
0.09 mass% RuO_2	T_L	931	1309
Repeated Measurement,	T_{M2}	1222	1233
0.03 mass% RuO_2	T_L	929	1296

(a) An outlier—see Section 5.3.2

6.2 Experimental Error Assessment

Liquidus temperature measurement is subject to several sources of possible errors. Suspected sources of errors are discussed below.

6.2.1 Batch Preparation

The maximum accepted weighing error was 0.03%, i.e., 0.15 g for 450 g of glass. The actual weight of batches was 0.01 to 0.10 g lower than the theoretical weight for 450 g of glass. Additionally, a glass batch undergoes several operations, such as mixing and milling, during which some batch components may selectively be lost into dust or attached to containers and equipment. Great care was made to minimize these losses. More than 100 glasses were analyzed in the CVS study [14], and the analyzed-batched composition differences were statistically evaluated. Some instances of analytical biases were identified; for example, SiO_2 analytical values were typically 3 to 4 mass% lower than as-batched values. No single instance of incorrect batching was detected.

6.2.2 Batch and Glass Mixing

Mixing and remelting glass batches minimized error due to chemical nonuniformity of glass. Any concentration inhomogeneity that brings a local enrichment of T_L increasing components (Cr, Ni) or impoverishment of T_L decreasing components (Na, Li) can produce a spinel crystal above the T_L of the bulk glass and thus result in an erroneous T_L value. Therefore,

great care is necessary in reducing glass inhomogeneity to a minimum. Interestingly, a spatially nonuniform distribution of spinel does not necessarily indicate chemical inhomogeneity. Spinel is rarely distributed evenly in the glass matrix. It precipitates in layers, probably due to the Liesegang effect or because of agglomeration in a velocity gradient [22,29].

Based on experience, we believe that glass batching, mixing, and melting variations are minor contributions to variations in T_L values.

6.2.3 Temperature Measurement

Error associated with the thermocouple positioning in the furnace and temperature fluctuation in the laboratory was within ±3°C to ±5°C. Additional error was associated with heat-treating samples in more than one furnace. This was necessitated by performing more than 400 heat-treatments within 15 weeks, i.e., 4 to 5 heat-treatments daily. Five furnaces were used for heat-treatment, two for nonradioactive glasses, and three for glasses with uranium. The error introduced this way was minimized by measuring the temperature at the position of the sample using calibrated thermocouples and by using a correction based on the SP-1 internal standard glass. The accuracy of corrected measurements was checked using an NBS standard glass in each furnace. This procedure is described in Section 3.3.7.

Some fraction of the differences in unadjusted T_L values of the standard glass in different furnaces can be attributed to the thermocouple variation and the standard glass variation. The main source of these differences is the temperature difference between the thermocouple and the glass sample caused by the differences in heat transfer from heating elements to the thermocouple and to the sample.

6.2.4 Volatilization During Melting

Volatilization during melting was minimized by using a lid on the crucible. Because of the high Henry's constant (approximately 10^9), the lid keeps nearly saturated vapors above the melt, thus effectively reducing the rate of vaporization. The CVS study [14] of more than 100 glasses shows no evidence of alkali or B_2O_3 depletion by volatilization during melting. The same conclusions were made in a recent study, in which triplicate independent chemical analyses of 10 HLW glasses were performed.

Chemical analyses of DWPF glasses will be performed at SRTC. Only one glass was chemically analyzed in this study. Table 6.3 displays chemical analyses of SG06 glass melted at 1150°C and remelted at 1322°C.

Table 6.3. As-batched and Analytical Compositions of SG06 Glass

Oxide	Target	1150°C[(a)]	Δ, %[(b)]	1322°C[(c)]	Δ, %[(b)]
SiO_2	.4991	.4660	-7	.4920	-1
B_2O_3	.0500	.0530	6	.0530	6
Al_2O_3	.0799	.0890	11	.0850	6
Li_2O	.0300	.0300	0	.0305	2
Na_2O	.1099	.1200	9	.1100	0
K_2O	.0380	.0445	17	.0446	17
MgO	.0050	.0054	8	.0051	2
CaO	.0200	.0233	17	.0226	13
MnO	.0100	.0097	-3	.0097	-3
NiO	.0005	.0005	0	.0006	20
Fe_2O_3	.1499	.1390	-7	.1390	-7
Cr_2O_3	.0010	.0015	50	.0016	60
TiO_2	.0060	.0059	-2	.0060	0
RuO_2	.0009	(d)		(d)	
Sum	1.0000	.9878		.9997	

(a) Analyzed composition of glass melted at 1150°C.
(b) The relative difference between analyzed and batched mass fraction.
(c) Analyzed composition of glass melted at 1322°C.
(d) Ru concentration was not measured.

Both analyses show higher (up to 17%) than as-batched concentrations of most components. Only SiO_2, Fe_2O_3, and MnO analytical values are lower than as-batched values. These differences are within a typical analytical error of 6 to 14% for most components, except two minor components, Cr_2O_3 and NiO. In particular, no depletion of alkali or B_2O_3 was detected for the glass melted for 2 h either at 1150°C (the first melt) or 1322°C (the second melt).

Based on chemical analyses of numerous glasses in CVS [14] and other studies, as well as Table 6.3, volatilization during melting is expected to have no measurable effect on glass composition and thus no measurable effect on T_L. To check this, T_L was measured on glass SG13 that was melted at 1319°C for 1 h and then remelted at 1400°C for 1 h. The T_L values were 1070°C (1319°C, 1h) and 1063°C (1400°C, second melt, 1 h). This difference is within experimental error and is opposite to an expected effect of alkali and boron evaporation (see

Sections 6.1.10 and 6.1.11). However, alkali evaporation could affect T_L values that are high above T_5. Therefore, shorter heat-treatment time is necessary for these glasses—see the following section.

6.2.5 Volatilization During Heat-treatment

Employing the uniform temperature method substantially reduced the effect of volatilization on crystallization during heat-treatment. The gradient temperature method should not be used for HLW glass at temperatures > 1000°C because of convection currents driven by surface tension gradients induced by volatilization (its effect is felt at temperatures as low as 850°C). The perforated-plate method uses samples with a large surface-volume ratio, and thus is also susceptible to compositional changes by volatilization, especially for glasses with surface crystallization. However, this is an efficient method for a rough estimate of T_L before the uniform temperature measurement in a closed box. The method used in this work reduced, but did not fully eliminate, the effects of volatilization during heat-treatment.

Volatilization depletes alkali borates in the meniscus area, more strongly at temperatures above 1200°C, resulting in a local increase of T_L (alkali oxides reduce T_L). The crystals formed in the meniscus are carried by convection into the bulk melt, where they tend to redissolve, and can be recognized by rounded edges. The extent of this volatilization-induced crystallization increases with increasing heat-treatment temperature and time. It was substantially reduced by heat-treating high-temperature samples (>1200°C) for shorter times, 1 to 3 h (Section 3.3.6); 1 h was sufficient at T > 1200°C for establishing redox equilibrium and much longer than the time needed for phase equilibrium.

6.2.6 Effect of RuO_2

An effort was made to reduce undissolved RuO_2 in glass by increasing the melting temperature (Section 3.2.1). A high density of RuO_2 particles and agglomerates made the detection of spinel crystals difficult or impossible in some glasses when spinel concentration was low near T_L (see Section 3.3.1). Evidence exists that a part of the dissolved RuO_2 could become a spinel component (see Sections 4.2 and 6.1.9), and thus RuO_2 could affect T_L. Further attention to the effect of RuO_2 on T_L is, therefore, recommended.

6.2.7 Redox

The redox state of glass at $p_{O_2} = const.$ is a function of temperature [30]. Batches were melted using Fe_2O_3 as a source of iron, which is usually reduced by 3 to 5% to FeO at 1150°C, probably at equilibrium with O_2 bubbles that are produced by the chemical reaction

$$2Fe_2O_3 \rightarrow 4FeO + O_2 \qquad (6)$$

This reaction is as vigorous as other glass-fining reactions and may cause foaming.

In this work, glasses were melted at temperatures from 1107°C (SG01) to 1400°C (SG13), and thus their redox state varied accordingly. During heat-treatment, which occurred at a substantially lower temperature than that at which glasses were prepared, the glass had a tendency to oxidize. As explained in Section 3.3.4, T_L was measured when samples were at equilibrium with atmospheric air. The effect of melter redox can be determined by heat-treating glass under a controlled atmosphere with varied p_{O_2}.

6.2.8 Overall Estimate of Error in Reported T_L Values

The Validation Section asserts that the error in measured T_L values was approximately ±12°C. Of this, ±5°C was attributed to the temperature measurement error, ±5°C, to the error associated with furnace calibration using a standard glass, and the rest to other causes. Glass preparation and melt-volatilization are unlikely sources of a major error. Alkali volatilization during heat-treatment could be a source of error only for glasses with a high T_L. The presence of a high concentration of RuO_2 can cause error of an unknown magnitude. Some error can be associated with the uncertainty of the glass redox-state at T_L.

7.0 References

1. Westinghouse Savannah River Company. 1996. *High-level Waste System Plan*, Revision 7, HLW-OVP-96-0083, Aiken, South Carolina.

2. U.S. Department of Energy. 1996. *Integrated Data Base Report – 1995: U.S. Spent Nuclear Fuel and Radioactive Waste Inventories, Projections, and Characteristics*, DOE/RW-0006, Rev. 12, Washington DC.

3. C. M. McConville, M. E. Johnson, and S. L. Derby. 1995. *Decision Analysis Model for Assessment of Tank Waste Remediation System Waste Treatment Strategies*, WHC-EP-0874, Westinghouse Hanford Company, Richland, Washington.

4. P. Hrma and P. A. Smith. 1994. "The Effect of Vitrification Technology on Waste Loading," *Proc. Int. Top. Meeting Nucl. Hazard. Waste Manag. Spectrum '94*, Vol. 2, pp. 862-867.

5. P. Hrma. 1994. "Toward Optimization of Nuclear Waste Glasses: Constraints, Property Models, and Waste Loading," *Ceram. Trans.* 45, 391-401.

6. D.-S. Kim and P. Hrma. 1994. "Development of High-Waste Loaded High-Level Nuclear Waste Glasses for High Temperature Melter," *Ceram. Trans.* 45, 39-47.

7. P. T. Fini and P. Hrma. 1994. "Maximization of Waste Loading for a Vitrified Hanford High-Activity Simulated Waste," *Ceram. Trans.* 45, 49-57.

8. P. Hrma, J. D. Vienna, and M. J. Schweiger. 1996. "Liquidus Temperature Limited Waste Loading Maximization for Vitrified HLW," *Ceram. Trans.* 72, 449-456.

9. J. D. Vienna, P. R. Hrma, M. J. Schweiger, D. E. Smith, and D. S. Kim. 1995. *Low-Temperature High-Waste Loading Glass for Hanford DST/SST High-Level Waste Blend - Technical Note*, PNNL-11126, Pacific Northwest Laboratory, Richland, Washington.

10. S. L. Lambert, G. E. Stegen, and J. D. Vienna. 1996. *Tank Waste Remediation System Phase I High-Level Waste Feed Processability Assessment Report*, WHC-SD-WM-TI-768, Westinghouse Hanford Company, Richland, Washington.

11. C. M. Jantzen. 1991. "First Principals Process-Product Models for Vitrification of Nuclear Waste: Relationship of Glass Composition to Glass Viscosity, Resistivity, Liquidus Temperature, and Durability," *Ceram. Trans.* 23, 37-51.

12. K.-S. Kim, D. K. Peeler, and P. Hrma. 1995. "Effects of Crystallization on the Chemical Durability of Nuclear Waste Glasses," *Ceram. Trans.* 61, 177-185.

13. P. Hrma and R. J. Robertus. 1993. "Waste Glass Design Based on Property Composition Functions," *Ceram. Eng. Sci. Proc.* 14 [11-12] 187-203.

14. a) P. Hrma, G. F. Piepel, M. J. Schweiger, D. E. Smith, D.-S. Kim, P. E. Redgate, J. D. Vienna, C. A. LoPresti, D. B. Simpson, D. K. Peeler, and M. H. Langowski. 1994. *Property / Composition Relationships for Hanford High-Level Waste Glasses Melting at 1150°C,* PNL-10359, Vol. 1 and 2, Pacific Northwest Laboratory, Richland, Washington; b) P. Hrma, G. F. Piepel, P. E. Redgate, D. E. Smith, M. J. Schweiger, J. D. Vienna, and D.-S. Kim. 1995. "Prediction of Processing Properties for Nuclear Waste Glasses," *Ceram. Trans.* 61, 505-513.

15. M. Mika, M. J. Schweiger, and P. Hrma. 1997. "Liquidus Temperature of Spinel Precipitating High-Level Waste Glass," *Scientific Basis for Nuclear Waste Management* (Editors W. J. Gray and I. R. Triay), Vol. 465, p. 71-78, Material Research Society, Pittsburgh, Pennsylvania.

16. K.-S. Kim and P. Hrma. 1994. "Models for Liquidus Temperature of Nuclear Waste Glasses," *Ceram. Trans.* 45, 327-337.

17. J. G. Reynolds and P. Hrma. 1997. "The Kinetics of Spinel Crystallization from a High-Level Waste Glass," *Scientific Basis for Nuclear Waste Management* (Editors W. J. Gray and I. R. Triay), Vol. 465, p. 65-70, Material Research Society, Pittsburgh, Pennsylvania.

18. C. M. Jantzen, and K. B. Brown. 1993. "Statistical Process Control of Glass Manufactured for Nuclear Waste Disposal," *Bull. Am. Ceram. Soc.* 72 [5] 55-59.

19. J. D. Vienna, P. Hrma, D. S. Kim, M. J. Schweiger, and D. E. Smith. 1996. "Compositional Dependence of Viscosity, Electrical Conductivity, and Liquidus Temperature of Multicomponent Borosilicate Waste Glasses," *Ceram. Trans.* 72, 427-436.

20. A. D. Cozzi, D. K. Peeler, and C. M. Jantzen. 1996. *Scoping Study to Evaluate Liquidus Temperature Measurements Performed by PNNL and CELS* (Draft), Westinghouse Savannah River Company, Savannah River Technology Company, Aiken, South Carolina.

21. W. T. Cobb and P. Hrma. 1991. "Behavior of RuO_2 in a Glass Melt," *Ceram. Trans.* 23, 233-237.

22. M. J. LaMont and P. Hrma. 1998. "A Crucible Study of Spinel Settling in a High-Level Waste Glass," *Ceram. Trans.*87, 343-348.

23. A. D. Pelton, P. Wu, G. Eriksson, and S. Degtiarev. 1996. "Development of Models and Software for Liquidus Temperatures of Glasses of HWVP Products," PNNL-11037, UC-810, Pacific Northwest National Laboratory, Richland, Washington.

24. C. J. Capobianco and M. J. Drake. 1990. "Partitioning of Ruthenium, Rhodium, and Palladium between Spinel and Silicate Melt and Implications for Platinum Group Element Fractionation Trends," *Geochem. Cosmochim. Acta* 54, 869-874.

25. P. Hrma and R. J. Robertus. 1993. "Waste Glass Design Based on Property Composition Functions," *Ceram. Eng. Sci. Proc.* 14 [11-12] 187-203.

26. D. F. Bickford, and C. M. Jantzen. 1986. "Devitrification of Defense Nuclear Waste Glasses: Role of Melt Insolubles," *J. Non-Crystalline Solids* 84 [1-3] 299-307.

27. D-S. Kim, P. Hrma, D. E. Smith, and M. J. Schweiger. 1994. "Crystallization in Simulated Glasses from Hanford High-Level Nuclear Waste Composition Range," *Ceram. Trans.* 39, 179- 189.

28. H. D. Schreiber, F. A. Settle, P. L. Jamison, J. P. Eckenrode, and G. W. Headley. 1986. "Ruthenium in Glass-forming Borosilicate Melts," *J. Less-Common Metals*, 115, 145-154.

29. M. J. Schweiger, M. W. Stachnik, and P. Hrma. 1998. "West Valley High-Level Waste Glass Crystallization in Canisters," *Ceram. Trans.*87, 335-341.

30. H. D. Schreiber, S. J. Kozak, A. L. Fritchman, D. S. Goldman, and H. A. Schreiber. 1986. "Redox Kinetics and Oxygen Diffusion in a Borosilicate Melt," *Phys. Chem. Glasses* 27 [4] 152-177.

31. J. D. Vienna, P. Hrma, and D. E. Smith. 1997. "Isothermal Crystallization Kinetics in Simulated High-Level Nuclear Waste Glass," *Scientific Basis for Nuclear Waste Management* (Editors W. J. Gray and I. R. Triay), Vol. 465, p. 17-24, Material Research Society, Pittsburgh, Pennsylvania.

32. G. F. Piepel, C. M. Anderson, and P. E. Redgate. 1993. "Response Surface Designs for Irregularly-Shaped Regions" (Parts 1, 2, and 3), *1993 Proceedings of the Section on Physical and Engineering Sciences*, 205-227, American Statistical Association, Alexandria, Virginia.

33. H. Li, P. Hrma, M. H. Langowski, J. Hlavac, O. Vojtech, V. Krestan, and P. Exnar. 1996. "Vitrification and Chemical Durability of Simulated High-Level Nuclear Waste Glasses with High Concentrations of Cr_2O_3 and Al_2O_3," *Ceram. Trans.* 72, 299-306.

Distribution

No. of Copies

OFFSITE

2 U.S. DOE / Office of Scientific and Technical Information

1 DOE Savannah River Operations Office
P.O. Box A
Aiken, South Carolina 29802
Attn: T. S. Gutmann

6 Westinghouse Savannah River Co.
SRTC, Bldg 773-A
Aiken, South Carolina 29808
Attn: K. G. Brown
E. W. Holtzscheiter
C. M. Jantzen
S. L. Marra
J. P. Morin
D. K. Peeler

FOREIGN

1 Department of Silicates
Institute of Chemical Technology
Technicka 5
166 28 Praha
Czech Republic
Attn: M. Mika

No. of Copies

ONSITE

2 DOE Richland Operations Office
P. O. Box 550, MS: K8-50
Richland, Washington 99352
Attn: T. P. Pietrok K8-50
C. S. Louie A0-21

4 PHMC, Hanford
Attn: J. O. Honeyman R2-58
R. M. Orme R3-73
D. L. Penwell R3-73
R. S. Wittman R3-73

43 Pacific Northwest National Laboratory
W. F. Bonner K9-14
J. L. Buelt K9-09
J. V. Crum K6-24
P. Hrma (20) K6-24
H. Li K6-24
E. V. Morrey P7-28
J. M. Perez A0-21
L. M. Peurrung K6-24
G. F. Piepel K5-12
M. J. Schweiger K6-24
J. D. Vienna K6-24
B. J. Williams (TFA) (8) K9-69
Technical Report Files (5) P8-55